

Article

## Estimation of Actual Crop Coefficients Using Remotely Sensed Vegetation Indices and Soil Water Balance Modelled Data

Isabel Pôças <sup>1,2,\*</sup>, Teresa A. Paço <sup>1</sup>, Paula Paredes <sup>1</sup>, Mário Cunha <sup>2,3</sup> and Luís S. Pereira <sup>1</sup>

<sup>1</sup> LEAF—Linking Landscape, Environment, Agriculture and Food, Instituto Superior de Agronomia, Universidade de Lisboa, Tapada da Ajuda, 1349-017 Lisboa, Portugal;

E-Mails: tapaco@isa.utl.pt (T.A.P.); pparedes@isa.utl.pt (P.P.); lspereira@isa.utl.pt (L.S.P.)

<sup>2</sup> Centro de Investigação em Ciências Geo-Espaciais (CICGE), Rua do Campo Alegre, 4169-007 Porto, Portugal; E-Mail: mcunha@mail.icav.up.pt

<sup>3</sup> Faculdade de Ciências da Universidade do Porto, Rua do Campo Alegre, 4169-007 Porto, Portugal

\* Author to whom correspondence should be addressed; E-Mail: ipocas@mail.icav.up.pt; Tel.: +351-220-402-160; Fax: +351-220-402-490.

Academic Editors: Gabriel Senay and Prasad S. Thenkabail

Received: 25 October 2014 / Accepted: 15 February 2015 / Published: 27 February 2015

---

**Abstract:** A new procedure is proposed for estimating actual basal crop coefficients from vegetation indices ( $K_{cb\ VI}$ ) considering a density coefficient ( $K_d$ ) and a crop coefficient for bare soil.  $K_d$  is computed using the fraction of ground cover by vegetation ( $f_c\ VI$ ), which is also estimated from vegetation indices derived from remote sensing. A combined approach for estimating actual crop coefficients from vegetation indices ( $K_c\ VI$ ) is also proposed by integrating the  $K_{cb\ VI}$  with the soil evaporation coefficient ( $K_e$ ) derived from the soil water balance model SIMDualKc. Results for maize, barley and an olive orchard have shown that the approaches for estimating both  $f_c\ VI$  and  $K_{cb\ VI}$  compared well with results obtained using the SIMDualKc model after calibration with ground observation data. For the crops studied, the correlation coefficients relative to comparing the actual  $K_{cb\ VI}$  and  $K_c\ VI$  with actual  $K_{cb}$  and  $K_c$  obtained with SIMDualKc were larger than 0.73 and 0.71, respectively. The corresponding regression coefficients were close to 1.0. The methodology herein presented and discussed allowed for obtaining information for the whole crop season, including periods when vegetation cover is incomplete, as the initial and development stages. Results show that the proposed methods are adequate for supporting irrigation management.

**Keywords:** actual basal crop coefficient; evapotranspiration; evaporation coefficient; fraction of ground cover; remote sensing; NDVI; SAVI; SIMDualKc model; water stress coefficient

---

## 1. Introduction

The accurate estimation of crop water requirements plays an important role in the improvement of crops water use and irrigation performance. This issue is particularly relevant considering the need for intensification of irrigated agriculture and increased water scarcity in several regions of the world.

A common approach for the estimation of crop water requirements is the  $K_c$ - $ET_o$  approach adopted by FAO56 [1] where a reference crop evapotranspiration ( $ET_o$ ) is multiplied by a crop coefficient ( $K_c$ ) for estimating crop evapotranspiration,  $ET_c$ . The  $ET_o$  represents the climatic demand of the atmosphere while the  $K_c$  represents the differences distinguishing the reference crop and the considered crop in terms of ground cover, canopy properties and aerodynamic resistance, thus in terms of crop ET. Alternatively, crop evapotranspiration may be computed directly from ground observations using a combination equation such as the Penman-Monteith equation [2,3]. However, this approach is more demanding than the  $K_c$ - $ET_o$  approach and is not used for operational purposes but limited to research.

Another approach for estimating crop ET is based on surface energy balance models that use remote sensing thermal infrared data (e.g., [4–6]). These models estimate crop ET by subtracting the soil heat flux ( $G$ ) and sensible heat flux ( $H$ ) from the net radiation ( $R_n$ ) at the surface. Such models allow to directly integrating the effects related with soil water deficit or water vapor pressure in the crop ET estimation [7]. Crop coefficients can be further derived considering the  $ET_o$  [8–10]. However, these models present greater complexity and larger amount of input data than the  $K_c$ - $ET_o$  approach [7]. The  $K_c$ - $ET_o$  approach is commonly accepted for operational and research objectives [11]. A single or dual  $K_c$  approach may be used [1]. In the single approach both crop transpiration and soil evaporation are timely averaged into a single coefficient ( $K_c$ ), whereas in the dual approach a daily basal crop coefficient ( $K_{cb}$ ), representing primarily the plant transpiration, and a daily soil evaporation coefficient ( $K_e$ ) are considered separately, *i.e.*,  $K_c = K_{cb} + K_e$ .

For transferability purposes,  $K_c$ ,  $K_{cb}$  and  $ET_c$  in FAO56 represent ET rates under optimal, well-watered conditions [1]. However, in the field and in common practice, crop conditions are often not optimal due to insufficient or non-uniform irrigation, crop density, soil salinity and/or agronomic management. Potential  $ET_c$  must then be replaced by the actual  $ET_c$  ( $ET_{c\ act}$ ), and the resulting  $K_c$  is renamed  $K_{c\ act}$  and  $K_{cb}$  is also renamed  $K_{cb\ act}$  [11]. The term actual is adopted in this study. As commented by Pereira *et al.* [11], this concept better supports estimation and transferability avoiding the need to define multiple  $K_c$  values for the same crop as has occurred in the past for several crops, e.g., vines and orchards. Moreover, adopting  $K_{c\ act}$  and  $K_{cb\ act}$  rather than using the potential crop coefficients allows to perform irrigation management closer to the actual conditions, which is a main motivation of the present study.

Standard, potential  $K_c$  and  $K_{cb}$  values are defined and tabulated for a wide range of agricultural crops [1,12], but appropriate corrections may be required adopting a stress coefficient ( $K_s$ ) to obtain

the actual  $K_c$  ( $K_{c \text{ act}} = K_s K_c$  or  $K_{cb \text{ act}} = K_s K_{cb}$ ). In addition, the transferability of  $K_c$  and  $K_{cb}$  values requires appropriate adjustment to local climate [1]. The adjustment of tabulated  $K_c$  and  $K_{cb}$  values for local conditions is also necessary when differences occur in planting density and geometry, vegetation height, and canopy architecture particularly in case of tree and vine crops [1,12].

In the last two decades, remote sensing (RS) data has increasingly been used for monitoring and mapping the spatial and temporal variation of ET and thus for computing crop water requirements (e.g., [13–15]). One of the most widely used approaches considers the relationship between vegetation indices (VI) derived from RS reflectance data and (actual) crop coefficients, either  $K_c$  or  $K_{cb}$ . The basis of this approach relies on the close correlation of several VI and various biophysical characteristics of the plants, e.g., leaf area index (LAI), ground cover fraction ( $f_c$ ), biomass, and physiological processes depending on light absorption by the canopy, including ET (e.g., [16–19]). With the VI approach, because these indices reflect the actual vegetation cover conditions, the estimated  $K_c$  or  $K_{cb}$  represent actual rather than potential  $K_c$  or  $K_{cb}$ . As proposed by Pereira *et al.* [11], these coefficients should then be referred to as  $K_{c \text{ act}}$  and  $K_{cb \text{ act}}$  despite many authors have not adopted this conceptual difference and that most VI-based methods are unable to accurately observe reductions in  $K_c$  and  $K_{cb}$  caused by acute water or salinity stress.

One advantage of using VI-based actual crop coefficients is the ability to account for variations in plant growth due to abnormal weather conditions, e.g., the impact of a frost occurrence [20]. Using VI-based crop coefficients also allows obtaining the spatial variation of actual  $K_c$  (or  $K_{cb}$ ) within fields. In addition they provide for a field-to-field description of the variation of actual  $K_c$  (or  $K_{cb}$ ) due to variations in planting dates, plant spacing and cultivars [11]. A review of the advantages and disadvantages of VI-based crop coefficients was presented by Allen *et al.* [21].

The Normalized Difference Vegetation Index (NDVI; [22]) and the Soil Adjusted Vegetation Index (SAVI; [23]) are the most commonly VI used to estimate actual  $K_c$  and  $K_{cb}$ . The formulation of both VI combines the reflected light in the red and near infrared (NIR) bands, thus providing an indirect measure of the absorption of red light by chlorophylls (a and b) and reflectance of NIR by the mesophyll structure in leaves [17,24]. Choudhury *et al.* [25] refer that using SAVI instead of NDVI allows extending the range over which the VI respond to the increase in vegetation amount/density beyond a LAI around 3, which is related with NDVI saturation problems for high LAI values. In addition, the NDVI is considered more sensitive than SAVI to soil background reflectance changes due to the moisture of soil surface [7,13,26].

Several relationships between  $K_{cb}$  (or  $K_c$ ) and VI are reported in the literature for different vegetation types, with the most recent studies focusing the  $K_{cb}$  estimation because plant transpiration is more directly related with the VI. Some examples of this approach consider a linear relationship between  $K_{cb}$  and NDVI [13,20,25,27,28], and between  $K_{cb}$  and SAVI [13,25,26] but an exponential relationship between NDVI and  $K_c$  was also considered [29]. A few studies report a  $K_{cb}$  estimation based on  $f_c$  or LAI obtained through VI, including for field and tree crops [7,30,31]. However, in most studies, the relationship between  $K_{cb}$  and VI was established for non-stressed conditions and for conditions of dry soil surface, which often do not represent the actual conditions of crop management. VI derived crop coefficients often do not account for the reduction in  $K_{cb}$  due to water or salinity stress [7,11]. Then the above referred stress coefficient  $K_s$  should be considered to obtain an actual  $K_c$  or  $K_{cb}$ , *i.e.*,  $K_{c \text{ act}}$  and  $K_{cb \text{ act}}$  [1]. Most of those studies were established for a single crop and its

application for other crops, particularly for discontinuous tree crops, is still limited. Differently, the approach proposed by Mateos *et al.* [7], which approximates  $K_{cb}$  using  $f_c$  and VI, refers to several crops and shows good results. However, this application does not always allow estimating  $K_{cb}$  for periods when the soil is not yet fully covered by the crop.

Although several equations were proposed for approaching  $K_{cb}$  via VI, a consensual equation that can be consistently used for different vegetation types and conditions is still lacking. In such context, a density coefficient ( $K_d$ ) [12] may be used in the formulation of  $K_{cb}$  through VI to help incorporating the impact of vegetation density and height. Such approach would allow  $K_{cb}$  to be computed for a range of row crops, orchards and vines, thus including conditions when soil is not fully covered by the crop. For further estimating  $K_c$ , a water balance modeling approach adopting the dual crop coefficient approach [1] is required to estimate soil evaporation and thus to estimate the evaporation coefficient  $K_e$  that can be combined with the VI based  $K_{cb}$ , *i.e.*,  $K_c = K_{cb} + K_e$ . The SIMDualKc model [32], which performs a daily water balance of the surface soil layer, provides for a daily  $K_e$ . Thus, by applying the dual coefficient approach and performing the soil water balance, the SIMDualKc model provides information on the stress coefficient  $K_s$ , on potential and actual  $K_{cb}$ , on  $K_e$  and ultimately on potential and actual  $K_c$ .

Considering the advances and limitations discussed above, particularly the need to represent actual rather than potential crop and evapotranspiration conditions for irrigation management purposes, the main objectives of this study are: (i) developing and testing a new equation for estimating actual  $K_{cb}$  based on VI and considering the stress coefficient  $K_s$  and the density coefficient  $K_d$  computed with the fraction of ground cover  $f_c$  estimated with VI; (ii) developing and testing a combined approach for estimation of the actual  $K_c$  using the VI-based  $K_{cb}$  and the evaporation coefficient  $K_e$  obtained with a daily soil water balance model; and (iii) testing the adequacy of the approach to different crop types, namely maize, barley, and an olive orchard.

## 2. Material and Methods

### 2.1. Study Areas

Three crops were considered to test the approach of actual  $K_c$  estimate based on reflectance VI in combination with the SIMDualKc soil water balance model: a super high density olive orchard, maize, and barley.

The super high density olive orchard test site is located in Viana do Alentejo, in South of Portugal (38°24'46" N, 7°43'38" W, 143 m a.s.l.; Figure 1). This olive orchard occupies a total area of 78 ha in an undulating terrain. The olive orchard was planted in 2006 in a hedgerow system with 1.35 m × 3.75 m spacing (1975 trees ha<sup>-1</sup>), and an orientation South-North. The olive trees are of cultivar Arbequina. The fraction of ground covered by the vegetation ( $f_c$ ) was approximately 0.35 and tree height was around 3.5 m. The procedure to obtain  $f_c$  was based upon the measurements of the projection of crown diameters in row direction and perpendicular to it in 51 trees. Soils are sandy loam, with soil water content averaging 0.24 cm<sup>3</sup>·cm<sup>-3</sup> at field capacity and 0.12 cm<sup>3</sup>·cm<sup>-3</sup> at the wilting point. Ground data from two consecutive years (2011 and 2012) were collected and used to validate information of several agronomic and biophysical parameters as detailed by Paço *et al.* [8] and Pôças *et al.* [33]. In 2012,

between February 20th and 25th, an extremely heavy frost affected the orchard causing a strong leaf fall. A severe pruning of the trees was therefore applied following the frost occurrence. Some areas of the olive orchard were more affected by the frost, and consequently the pruning was not uniform along the orchard, which increased the variability of the vegetation conditions within the orchard in 2012.

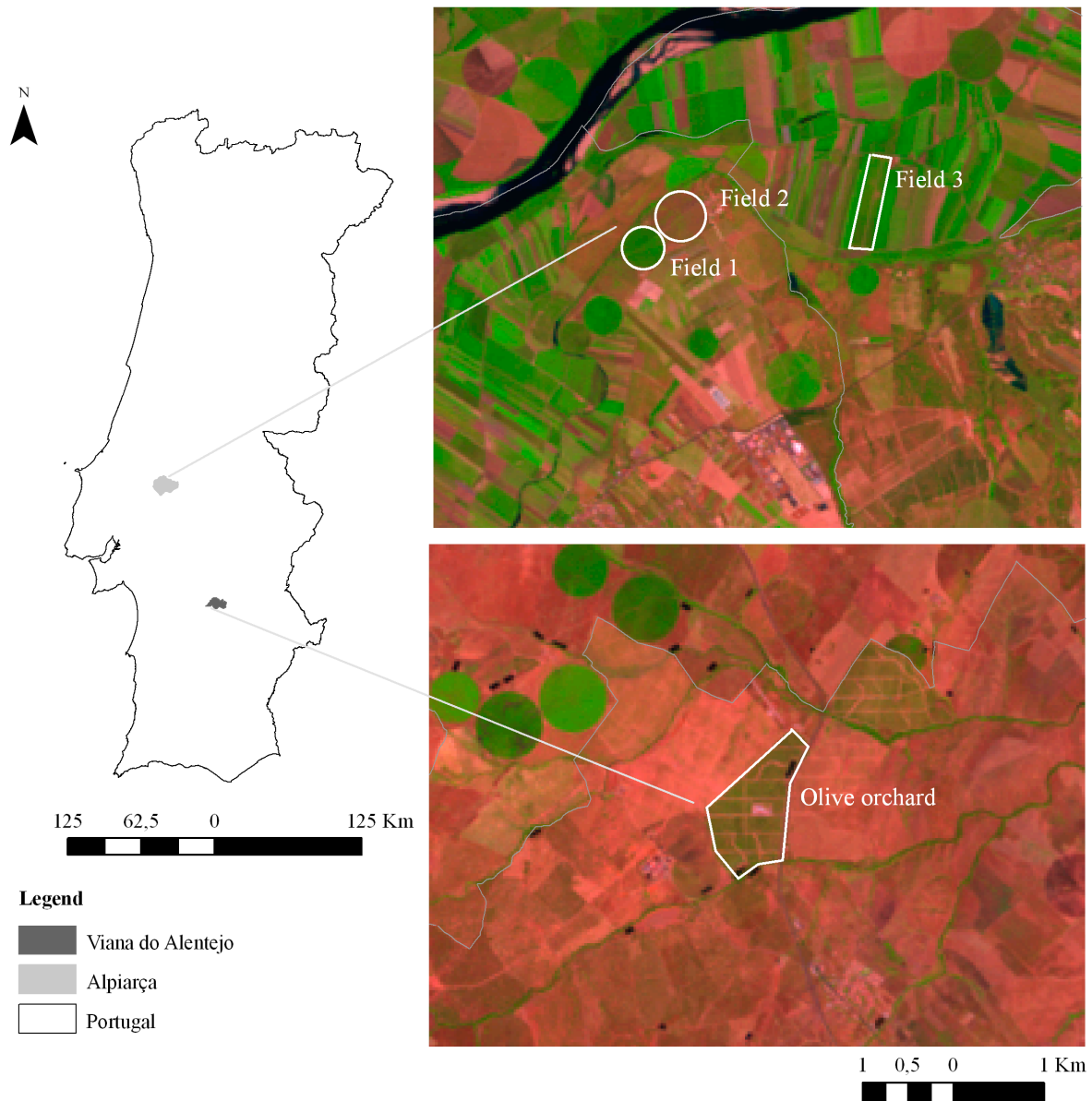


**Figure 1.** Study areas location in Viana do Alentejo and Alpiarça, Portugal.

Three farmer's fields of Quinta da Lagoalva de Cima located in Alpiarça, Ribatejo region, were surveyed for the maize crop [34]: (i) field 1 ( $39^{\circ}17'33''$  N,  $8^{\circ}34'19''$  W, 14 m a.s.l.); (ii) field 2 ( $39^{\circ}17'45''$  N,  $8^{\circ}34'01''$  W, 14 m a.s.l.); and (iii) field 3 ( $39^{\circ}18'04''$  N,  $8^{\circ}32'22''$  W, 16 m a.s.l.), (Figure 1). Fields have a cropped area of approximately 30 ha. In 2010, the maize was cropped in both fields 1 and 2, while in 2011 only field 1 was sowed; in 2012, fields 2 and 3 were cropped with maize. The PR33Y74 maize hybrid (FAO 600) was cultivated with a density of approximately  $82,000$  plants  $\text{ha}^{-1}$ . The length of each crop growth stages for all maize fields and seasons is described in Table 1. The crop growth stages were defined according to Allen *et al.* [1]: (i) initial stage, from the sowing/planting until 10%

of ground cover (Ini); (ii) development stage, from 10% of ground cover until maximum ground cover by vegetation (Dev); (iii) mid-season stage, from full cover until maturity (Mid), and (iv) late-season stage, from the beginning of senescence and leaves yellowing until harvesting (Late). The observations of  $f_c$  were visually performed and adjusted with the help of photographs of the ground shadow by the crop near solar noon [34].

Barley was sown in field 1; two seasons were studied: (i) 2012, a dry year, and (ii) 2012/2013, a wet year [35]. The barley field was cropped with  $200 \text{ kg} \cdot \text{ha}^{-1}$  of malting barley (Cv. Publican) seeds using an inter-row spacing of 0.15 m. The plants density was measured before tillering, when the crop attained tree leaves, averaging 342 and 319 plants per  $\text{m}^2$  respectively in 2012 and 2013. The lengths of the crop growth stages are given in Table 1. The barley  $f_c$  observations were performed similarly to the maize crop; furthermore, LAI measurements were also used to estimate  $f_c$  and therefore to confirm related observations as referred by Pereira *et al.* [35].

**Table 1.** Crop growth stages of maize and barley crops in each field and campaign.

Crop Growth Stages	Maize Study Areas	Barley Study Areas
	Field 1—Year 2010	2012 season
Initial (Ini)	25/05–25/06	16/01–06/02
Development (Dev)	26/06–22/07	07/02–03/04
Mid-season (Mid)	23/07–04/09	04/04–20/05
Late-season (Late)	05/09–13/10	21/05–26/06
	Field 2—Year 2010	2012/2013 season
Initial (Ini)	25/05–25/06	06/12–12/01
Development (Dev)	26/06–17/07	13/01–10/03
Mid-season (Mid)	18/07–02/09	11/03–05/05
Late-season (Late)	03/09–13/10	06/05–06/06
	Field 1—Year 2011	
Initial (Ini)	20/04–17/05	
Development (Dev)	18/05–28/06	
Mid-season (Mid)	29/06–17/08	
Late-season (Late)	18/08–20/09	
	Field 2—Year 2012	
Initial (Ini)	16/04–08/05	
Development (Dev)	09/05–24/06	
Mid-season (Mid)	25/06–20/08	
Late-season (Late)	21/08–20/09	
	Field 3—Year 2012	
Initial (Ini)	30/05–12/06	
Development (Dev)	13/06–15/07	
Mid-season (Mid)	16/07–13/09	
Late-season (Late)	14/09–12/10	

Soils in fields 1 and 2 are loamy sand soils, with total available water TAW = 171 and 149  $\text{mm} \cdot \text{m}^{-1}$  respectively; field 3 is a silty-loam soil, with TAW = 209  $\text{mm} \cdot \text{m}^{-1}$ . Ground data collected in maize and barley study areas included LAI and  $f_c$ , whose measurements were used to calibrate the SIMDualKc model as detailed by Paredes *et al.* [34] and Pereira *et al.* [35].

## 2.2. Satellite Imagery

Vegetation indices used for estimating the basal crop coefficients were obtained from Landsat 5 TM and Landsat 7 ETM+ satellite images. Landsat images of Path 203/Row 033 were considered for the olive orchard study area, while for the other study areas the Path 204/Row 033 was used. Table 2 presents the summary of the cloud-free satellite image dates considered for each study area and crop. The satellite image of 03 January 2013 was eliminated from the set of considered images due to the unfavorable light conditions during this period of the year, which affected the VI values.

**Table 2.** Satellite image dates considered for each study area and crop.

Olive Study Area (203/033)	Maize Study Areas (204/033)			Barley Study Areas (204/033)	
	Field 1	Field 2	Field 3	2012	2012–2013
31/01/2011 <sup>(1)</sup>	06/07/2010 <sup>(2)</sup>	06/07/2010 <sup>(2),*</sup>	11/07/2012 <sup>(2)</sup>	02/02/2012 <sup>(1)</sup>	03/01/2013 <sup>(1)</sup>
20/03/2011 <sup>(2)</sup>	22/07/2010 <sup>(3),*</sup>	22/07/2010 <sup>(3)</sup>	13/09/2012 <sup>(3)</sup>	18/02/2012 <sup>(2)</sup>	25/04/2013 <sup>(3)</sup>
05/04/2011 <sup>(2)</sup>	30/07/2010 <sup>(3),*</sup>	30/07/2010 <sup>(3),*</sup>	29/09/2012 <sup>(4)</sup>	05/03/2012 <sup>(2)</sup>	11/05/2013 <sup>(4)</sup>
23/05/2011 <sup>(3)</sup>	15/06/2011 <sup>(2)</sup>	11/07/2012 <sup>(3)</sup>		21/03/2012 <sup>(2)</sup>	
24/06/2011 <sup>(3)</sup>	25/07/2011 <sup>(3)</sup>	13/09/2012 <sup>(4)</sup>		24/05/2012 <sup>(4),*</sup>	
26/07/2011 <sup>(3)</sup>	18/08/2011 <sup>(3)</sup>				
27/08/2011 <sup>(3),*</sup>	19/09/2011 <sup>(4)</sup>				
12/09/2011 <sup>(3)</sup>					
06/10/2011 <sup>(4),*</sup>					
11/02/2012 <sup>(1)</sup>					
15/04/2012 <sup>(2),*</sup>					
20/07/2012 <sup>(3),*</sup>					
21/08/2012 <sup>(3),*</sup>					
06/09/2012 <sup>(3)</sup>					
08/10/2012 <sup>(4)</sup>					

<sup>(1)</sup> Ini; <sup>(2)</sup> Dev; <sup>(3)</sup> Mid; <sup>(4)</sup> Late (crop development stages). \* Dates when water stress occurrence was detected using the soil water balance model.

The images were geometrically and atmospherically corrected using the procedure described by Allen *et al.* [15] and Tasumi *et al.* [36]. The procedure included image calibration using the coefficients proposed in the literature for Landsat 5 TM and Landsat 7 ETM+ [37,38]. The VI were calculated on a pixel-by-pixel basis and averaged for the entire study plot in each study area. Pixels from the edges of the fields and from roads within the olive orchard were not considered. The VI computed for the study were the Normalized Difference Vegetation Index (NDVI; [22]) and the Soil Adjusted Vegetation Index (SAVI; [23]).

## 2.3. SIMDualKc

The SIMDualKc is a soil water balance model that applies the dual crop coefficient approach, thus separately computing the daily soil evaporation and crop transpiration [32,39]. This model has been successfully applied to estimate ET and assess  $K_c$  of a wide range of field crops [34,35,39], including tree crops [8,40]. Data from SIMDualKc were used as benchmark, *i.e.*, a standard against which

comparisons can be done, mainly for the comparison of  $K_c$  and  $K_{cb}$  results. SIMDualKc was previously calibrated using ground data for the three crops, as described later in this section.

In SIMDualKc,  $K_{cb}$  is computed with the equation below [12,32] where impacts of plant density and/or leaf area are taken into consideration by a density coefficient:

$$K_{cb} = K_{c \min} + K_d(K_{cb \text{ full}} - K_{c \min}) \quad (1)$$

where  $K_d$  is the crop density coefficient,  $K_{cb \text{ full}}$  is the estimated basal  $K_{cb}$  for peak plant growth conditions having nearly full ground cover (or LAI > 3), and  $K_{c \min}$  is the minimum  $K_c$  for bare soil (in the absence of vegetation). The  $K_{c \min}$  value is about 0.15 under typical agricultural conditions and ranges 0.0–0.15 for native vegetation depending on rainfall frequency.  $K_{cb}$  is adjusted by the model for local climatic conditions where the average minimum relative humidity differs from 45% and/or the average wind speed is different from  $2 \text{ m}\cdot\text{s}^{-1}$  [1,12,32].  $K_d$  is computed with the equation proposed by Allen and Pereira [12]:

$$K_d = \min\left(1, M_L f_{c \text{ eff}}, f_{c \text{ eff}}^{\left(\frac{1}{1+h}\right)}\right) \quad (2)$$

where  $f_{c \text{ eff}}$  is the effective fraction of ground covered or shaded by vegetation near solar noon [ ],  $M_L$  is a multiplier [ ] on  $f_{c \text{ eff}}$  describing the effect of canopy density on shading and on maximum relative ET per fraction of ground shaded (to simulate the physical limits imposed on water flux through the plant root, stem and leaf systems), and  $h$  is the mean height of the vegetation [m]. Therefore, the use of  $K_d$  allows incorporating the impact of vegetation density and height in the estimation of  $K_{cb}$ .  $K_d$  has also been used in other studies to adjust  $K_{cb}$  to actual density conditions for full cover crops [41] and in partial cover crops using both ground [42] or remote sensing data [43].

When soil water deficit occurs, the stress coefficient  $K_s$  [ ] is computed by the model using a daily soil water balance for the entire root zone.  $K_s$  is expressed as a linear function of the root zone depletion  $D_r$  [1,32]:

$$K_s = \frac{TAW - D_r}{TAW - RAW} = \frac{TAW - D_r}{(1-p)TAW}, \text{ for } D_r > RAW \quad (3)$$

$$K_s = 1, \text{ for } D_r \leq RAW \quad (4)$$

where TAW and RAW are, respectively, the total and readily available soil water [mm],  $D_r$  is the root zone depletion [mm], and  $p$  is the depletion fraction for no stress [ ].  $K_{cb}$  is multiplied by  $K_s$  to account for the effects of soil water stress and thus obtaining  $K_{cb \text{ act}}$ .

The calculation of the soil evaporation coefficient  $K_e$  [ ] follows the procedures proposed by [1,44] which include the daily water balance of the evaporation soil surface layer that allows to compute the evaporation reduction coefficient  $K_r$  [ ] from the cumulative depth of water depleted (evaporated) from the topsoil [1]. It results that  $K_e$  is then computed daily with:

$$K_e = K_r(K_{c \max} - K_{cb}) \leq f_{ew} K_{c \max} \quad (5)$$

as a function of  $K_{c \max}$ , the maximum value of  $K_c$  following rain or an irrigation event and  $K_{cb}$  in that day (Equation (1)) after adjustment with  $K_r$ .  $K_e$  is limited to  $f_{ew} K_{c \max}$  that represents the fraction of  $K_{c \max}$  that refers to the fraction  $f_{ew}$  of the soil that is both exposed and wetted, *i.e.*, the fraction of soil surface from which most evaporation occurs. The background and computation of  $K_{cb}$ ,  $K_s$  and  $K_e$  in SIMDualKc is described in detail by Rosa *et al.* [32].



The calibration of SIMDualKc aims at optimizing the crop parameters  $K_{cb}$  and  $p$  relative to the various crop growth stages, as well as the soil evaporation parameters, the deep percolation parameters, and the runoff curve number (CN) using trial and error procedures until small errors were achieved. Further information is provided by [8,34,35]. For the olive orchard, the calibration was performed comparing daily transpiration data simulated with those obtained with sapflow measurements (and also eddy covariance and energy balance measurements as auxiliary data for calibration and data quality screening), as described in Paço *et al.* [8]. For the maize and barley crops, the calibration was performed by minimizing the differences between observed and simulated soil water content, as described in Paredes *et al.* [34] and Pereira *et al.* [35]. In all cases, the results of goodness of fit indicators showed good model performance and small errors of estimates [8,34,35]. Furthermore, ET partitioning was performed in other studies, e.g., testing the soil evaporation algorithm through comparing simulated with microlysimeter observations [45,46], crop transpiration against sap flow measurements [8,40] and crop ET compared with eddy covariance ET data [47]. An example of the results of the model calibration for barley is presented in Figure 2, which shows that the simulated soil water content accurately follows the dynamics of observations throughout the barley crop season [35].

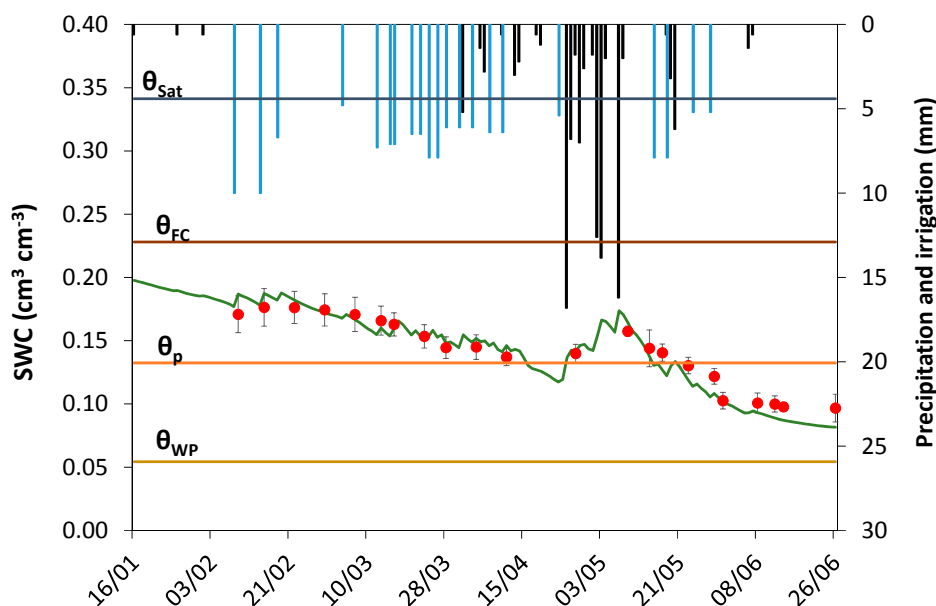


**Figure 2.** Observed (•) and simulated (—) daily soil water content (SWC) after the calibration of SIMDualKc for barley in the dry year (error bars correspond to the standard deviation of SWC observations);  $\theta_{Sat}$ ,  $\theta_{FC}$ ,  $\theta_p$  and  $\theta_{WP}$  are respectively the SWC at saturation, field capacity, wilting point and at non-stressed depletion fraction  $p$ ). Precipitation is represented by dark bars and irrigation by the light ones (source: [35]).

#### 2.4. Basal Crop Coefficients Derived from Reflectance Vegetation Indices

The proposed methodology is based on the dual crop coefficient approach, thus integrating daily  $K_{cb}$  and  $K_e$ , and considering  $K_s$  when water stress occurs [1,12]. Considering this approach, a new equation was developed to estimate  $K_{cb}$  from the density coefficient  $K_d$  and  $K_{c\ min}$  as proposed by Allen and Pereira [12] and from vegetation indices derived from satellite images,  $K_{cb\ VI}$ :

$$K_{cb\ VI} = K_{c\ min} + K_d \left( \frac{VI_i - VI_{min}}{VI_{max} - VI_{min}} \right) \quad (6)$$

where  $VI_i$  corresponds to the VI for a specific date and pixel,  $VI_{max}$  is the VI for maximum vegetation cover and  $VI_{min}$  is VI for minimum vegetation cover (bare soil). This equation adapts to crops with continuous ground cover and to tree crops with bare soil by including  $K_d$ . For tree crops having an active ground cover,  $K_{c\ min}$  is replaced by a  $K_{cb\ cover}$ , corresponding to the  $K_{cb}$  of the ground cover in the absence of tree foliage [12].  $K_d$  in Equation (6) is computed with Equation (2) using the effective fraction of ground covered estimated with the Equation (7) presented below. Table 3 presents  $K_d$  ranges for the three crops during the mid-season stage.

**Table 3.** Range of values of density coefficient computed for the satellite image dates of the mid-season stage in the three crops.

$K_d$	Maize Study Areas	Barley Study Areas <sup>(3)</sup>	Olive Study Areas
$K_d (f_{c\ field})$ <sup>(1)</sup>	[0.93–0.99]	0.90	[0.62–0.78]
$K_d (f_{c\ VI})$ <sup>(2)</sup>	[0.97–1.00]	0.90	[0.66–0.70]

<sup>(1)</sup>  $K_d$  computed using effective fraction of ground covered or shaded by vegetation derived from ground data;

<sup>(2)</sup>  $K_d$  computed using effective fraction of ground covered or shaded by vegetation estimated with vegetation indices using Equation (7); <sup>(3)</sup> A single value is presented because a single satellite image was available for the mid-season stage.

Both NDVI and SAVI vegetation indices may be used. The SAVI index is considered less sensitive to soil background reflectance variability than other VI, thus with higher potential for application in tree crops with discontinuous ground cover.  $NDVI_{max}$  was set to 0.75–0.85 for the three crops, and the value 0.10 was set for  $NDVI_{min}$ , both based on reference values for, respectively, an irrigated agricultural field with full cover and a bare soil [48–50]. When SAVI was considered, the  $SAVI_{min}$  was set to 0.09 while the  $SAVI_{max}$  was adjusted to 0.75 according to Mateos *et al.* [7].

The  $K_{c\ min}$  was set to a value between 0.10 and 0.15 (0.13 was considered in this study) according to values proposed by Allen and Pereira [12]. For the olive orchard,  $K_{cb\ cover}$  was considered instead of  $K_{c\ min}$  and set to a value between 0.15 and 0.18 (0.17 was considered in this study) due to the presence of sparse vegetation cover between tree rows. Reference values for several parameters considered in the computation of Equation (6) can be found in Allen and Pereira [12].  $K_d$  was computed with Equation (2) where, in a first approach, the  $f_{c\ eff}$  was the same considered in  $SIMDualKc$ , which was based in field observations ( $f_{c\ field}$ ). In a second approach,  $f_{c\ eff}$  was computed using an equation based on vegetation indices derived from remote sensing reflectance data ( $f_{c\ VI}$ ):

$$f_{c\ VI} = \beta_1 \left( \frac{VI_i - VI_{min}}{VI_{max} - VI_{min}} \right) + \beta_2 \quad (7)$$

where  $\beta_1$  is an empirical coefficient (ranging between 0 and 1) depending upon the maximum VI value in each crop stage.  $VI_i$  is the average VI of the study area pixels for each date,  $VI_{max}$  and  $VI_{min}$  correspond to the VI respectively for maximum and minimum vegetation cover. Both NDVI and SAVI may be used, with the latter producing better results for incomplete cover crops, e.g., olive orchards.  $NDVI_{max}$  and  $NDVI_{min}$  were set according to references in the literature [48–50] (Table 4). For the super high density olive orchard,  $SAVI_{max}$  and  $SAVI_{min}$  were considered following values proposed by

Mateos *et al.* [7] (Table 4). The parameter  $\beta_2$  corresponds to an adjustment coefficient associated with crop senescence and leaves yellowing. Both NDVI and SAVI are sensitive to leaf senescence thus yielding smaller values at the end of the growing cycle than before peak development was reached [51]. Therefore, the  $\beta_2$  adjustment is considered to compensate the decrease in VI due to the senescence and/or yellowing of plants, which is independent from  $f_c$ . Values of  $\beta_2$  are presented in Table 4.

**Table 4.** Values of parameters considered in the estimation of fraction of ground cover from vegetation indices.

Parameters	Crop Growth Stage	Value		
		Maize	Barley	Olive
NDVI <sub>max</sub>		0.75–0.85	0.75–0.85	0.75–0.85
NDVI <sub>min</sub>		0.1	0.1	0.1
SAVI <sub>max</sub>		0.75	0.75	0.75
SAVI <sub>min</sub>		0.09	0.09	0.09
$\beta_2$		0–0.5 <sup>(2)</sup>	0–0.5 <sup>(2)</sup>	0–0.5 <sup>(2)</sup>
$\beta_1$ <sup>(1)</sup>	Ini	0.3	0.3	0.4–0.7
	Dev	0.3–1	0.3–1	1
	Dev (1st sub-stage)	0.6	0.5	1
	Dev (2nd sub-stage)	0.9	0.7	-
	Dev (3rd sub-stage)	-	0.9	-
	Mid	1	1	-
	End	1	1	1

<sup>(1)</sup> The values were defined according to stages of the crop growth. For the development stage were considered sub-stages by dividing the growth stage in two (spring-summer crops; maize) or three (winter-spring crops; barley) periods; <sup>(2)</sup> 0 is considered when the crop is in its maximum development and 0.5 close to the harvest (a value of 0.2 was set in the first half of the late stage).

The four main stages of the crop growth, described by Allen *et al.* [1], were considered in the definition of  $\beta_1$ : (i) Ini, (ii) Dev, (iii) Mid, and (iv) Late. Due to the great variability of the ground cover by the vegetation throughout Dev, a differentiation of  $\beta_1$  values according to sub-stages was considered: (i) two sub-stages in spring-summer crops (maize); (ii) three sub-stages in winter-spring crops (barley), where the Dev is longer. For the olive orchard, a crop with persistent leaves and where the soil cover by the vegetation is incomplete, the  $\beta_1$  value was set to 1 throughout the year, except for the period of pruning and in the subsequent weeks, when it was slightly decreased to account for the decrease in canopies vegetation. Values of  $\beta_1$  are presented in Table 4.

Most of the optical VI track the effects of long-term water stress on plants but do not allow the early detection of water stress [52]. Therefore, Equation (6) expresses the potential  $K_{cb}$ , thus transpiration occurring at maximum rate. However, the occurrence of water stress cause a decrease of the potential value and  $K_s$  must be applied to obtain actual  $K_{cb}$  VI. In the current approach,  $K_s$  computed with SIMDualKc was used. The dates when water stress was detected through the daily soil water balance are given in Table 2. Therefore, hereafter, the actual  $K_{cb}$  VI refers to the  $K_{cb}$  VI computed by Equation (6) multiplied by the  $K_s$  computed with SIMDualKc.

For  $K_c$  estimation from VI, hereafter named  $K_{cVI}$ , the  $K_e$  computed with SIMDualKc was combined with the  $K_{cbVI}$ , *i.e.*,  $K_{cVI} = K_e + K_{cbVI}$ . A similar combined approach was reported by Mateos *et al.* [7]. The results of  $K_{cbVI}$  and  $K_{cVI}$  were compared with the actual  $K_{cb}$  and  $K_c$  computed with SIMDualKc based on field data, later referred as  $K_{cbSIMDualKc}$  and  $K_{cSIMDualKc}$ , respectively.

Because  $K_s$  and  $K_e$  used in the estimation of actual  $K_{cVI}$  are computed with SIMDualKc, the results of comparing actual  $K_{cVI}$  with  $K_{cSIMDualKc}$  are somehow influenced by the fact that values of  $K_s$  and  $K_e$  used in both cases are the same. Nevertheless, this fact does not impede the assessment of the computation of the actual  $K_{cbVI}$  because this is the procedure that gives the possibility to compare the actual crop coefficients from both approaches and retrieves useful information from satellite imagery aiming at irrigation management and farmer advising.

A linear regression forced through the origin was used for the comparisons and the corresponding regression and determination coefficients were consequently used as indicators. Additionally, the root-mean-square deviation (RMSD; Equation (8)) and the relative mean deviation (RMD; Equation (9)) were used to compare two sets of data, with  $X_i$  relative to estimations with SIMDualKc, having mean  $\bar{X}$ , and  $Y_i$  relative to the VI estimates ( $i = 1, 2, \dots, n$ ).

$$RMSD = \sqrt{\frac{\sum_{i=1}^n (X_i - Y_i)^2}{n}} \quad (8)$$

$$RMD = \frac{1}{n} \sum_{i=1}^n \frac{|X_i - Y_i|}{\bar{X}} \cdot 100 \quad (9)$$

Since the database available for this study only comprises 15 VI observations for maize and olive and seven for barley (Table 2), the validation of  $K_{cb}$  estimated based on VI was performed using the “leave-one-out” (LOO) cross-validation [53]. Applications of the LOO cross-validation in remote sensing studies are provided by [54,55]. The LOO cross-validation evaluates the model performance for observations not considered in the estimation step, thus providing independent estimates of the predictive capability of the selected models. This technique consists in the removal of one observation from the dataset used and the estimation of a new regression model with the remaining observations. This new regression model is used to estimate the  $K_{cbVI}$  of the observation withdrawn ( $K_{cbVILOO}$ ). Equations (8) and (9) were also used to estimate the goodness of cross-validation results, with  $X_i$  and  $Y_i$  representing respectively  $K_{cbSIMDualKc}$  and  $K_{cbVILOO}$  data. A similar approach was considered for the  $K_c$  and  $f_c$  estimated based on VI.

### 3. Results

#### 3.1. Estimation of the Fraction of Ground Cover from VI

The results of  $f_c$  estimated from NDVI ( $f_{cVI}$ ; Equation (7)) were compared with  $f_c$  based on field observations ( $f_{cfield}$ ) for the maize and barley crops (Figure 3). The comparison of  $f_{cVI}$  and  $f_{cfield}$  have shown a good agreement for both crops, with  $R^2 \geq 0.81$  and the regression coefficient  $b$  close to 1.0 (Figure 3). For maize, RMSD was 0.10 and RMD 10.6%, while for barley RMSD was 0.06 and RMD was 8.1%.

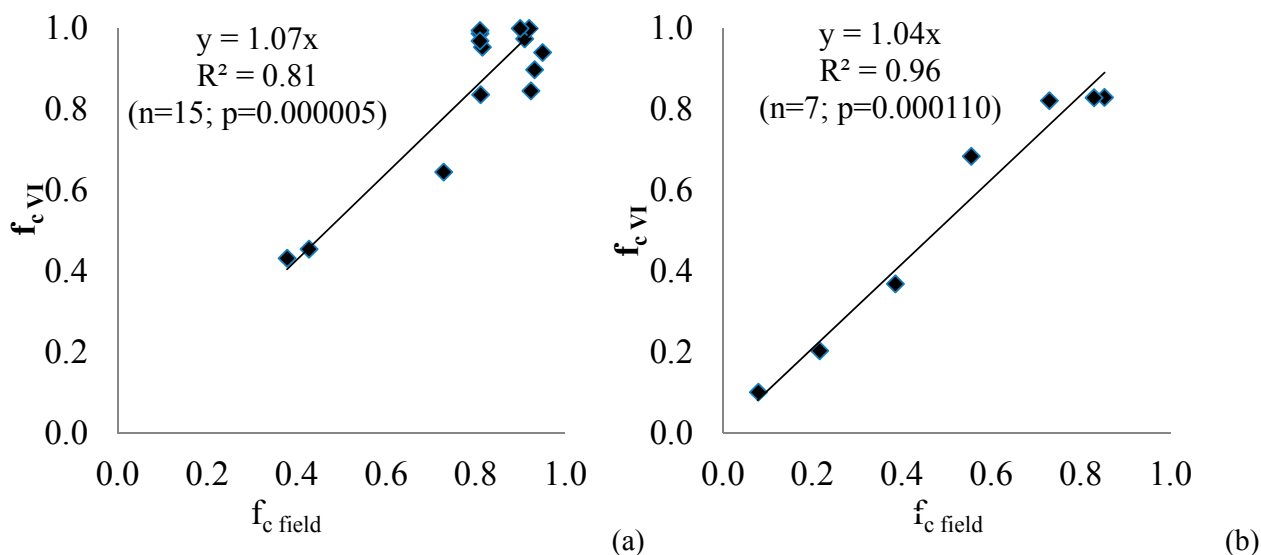


**Figure 3.** Comparison of the fraction of ground cover by vegetation derived from NDVI ( $f_{c\ VI}$ ) with the  $f_c$  obtained from field observations ( $f_{c\ field}$ ) for (a) maize and (b) barley.

For the olive crop, due to the low variability of  $f_{c\ field}$  values, a regression for comparing  $f_{c\ VI}$  and  $f_{c\ field}$  was not considered. The fraction of ground cover for this tree crop with persistent leaves is nearly constant throughout the year, except for the pruning period. As such, for the analysis of the  $f_{c\ VI}$  results, only the indicators of residual estimation deviations were used: RMSD = 0.22 and RMD = 69.2%. When SAVI was used for the estimation of  $f_{c\ VI}$  results of all indicators improved much, with RMSD= 0.02 and RMD = 5.5%. The absolute mean differences between the  $f_{c\ VI}$  and the  $f_{c\ field}$  for the olive orchard were small, ranging from 0.003 to 0.046. Contrarily, for the annual crops (maize and barley), the use of SAVI in the estimation of  $f_{c\ VI}$  did not improve the residual estimation deviations.

Results of cross validation show a good performance of the  $f_{c\ VI}$  estimation, with RMSD of 0.06, 0.04, and 0.01 respectively for maize, barley and olive. RMD results for the cross validation varied between 2.6% for olive and 7.5% for maize.

### 3.2. Estimation of $K_{cb}$ from Reflectance-Based Vegetation Indices ( $K_{cb\ VI}$ )

The  $K_{cb\ VI}$  (Equation (6)) was adjusted using the  $K_s$  derived from SIMDualKc computations for the dates when stress occurred (Table 2) to obtain the actual  $K_{cb\ VI}$ . The values of  $K_{cb\ SIMDualKc}$  used in comparisons with  $K_{cb\ VI}$  were also adjusted to water stress using  $K_s$ . Both NDVI and SAVI were tested for the estimation of  $K_{cb\ VI}$  and the results obtained with the two VI were compared.

The comparison of actual  $K_{cb\ VI}$  with actual  $K_{cb\ SIMDualKc}$  for the studied crops is presented in Figure 4. The  $K_{cb\ VI}$  values in Figure 4 were estimated using  $f_{c\ NDVI}$  (Equation (7)) with the objective of fully estimating actual  $K_{cb}$  from reflectance-based vegetation indices. Figure 4a shows  $K_{cb\ VI}$  for maize when using NDVI, which has a determination coefficient ( $R^2$ ) lower than using SAVI (Figure 4b) but has a higher regression coefficient ( $b = 0.98$ ) relative to SAVI (Table 5). Thus,  $K_{cb\ SAVI}$  underestimates  $K_{cb}$  values. For barley (Figure 4c,d) both  $b$  and  $R^2$  are better when using NDVI (Table 5). For the olive orchard estimating  $K_{cb\ VI}$  with SAVI leads to  $b$  equal to 1.22 and a  $R^2$  equal to 0.83; when using NDVI there is an overestimation of the  $K_{cb}$  values,  $b = 1.8$  (Figure 4e,f).

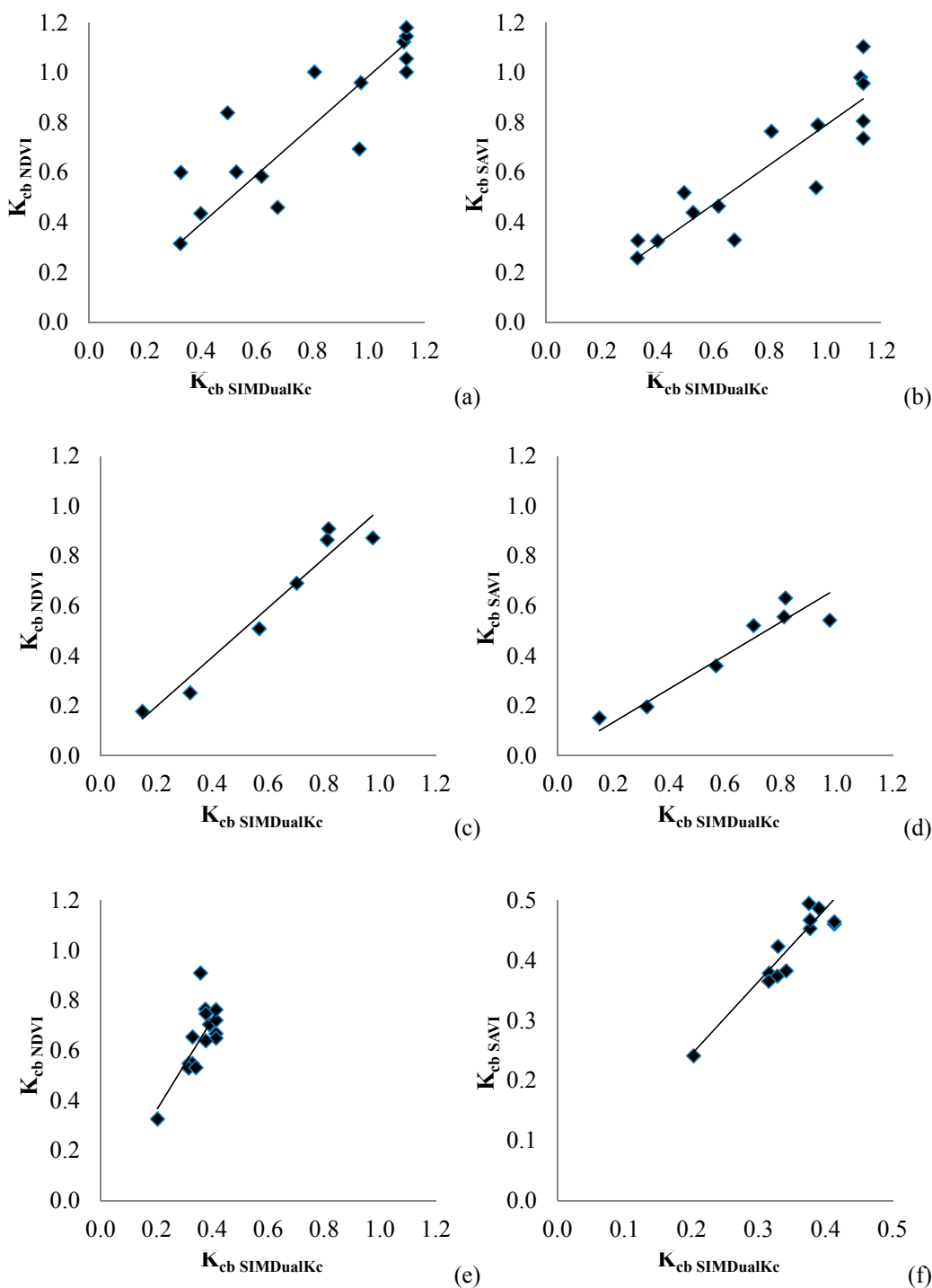


**Figure 4.** Comparison of actual  $K_{cb}$  derived from NDVI ( $K_{cb\ NDVI}$ ), on left, or from SAVI ( $K_{cb\ SAVI}$ ), on right, with the actual  $K_{cb}$  obtained with SIMDualKc ( $K_{cb\ SIMDualKc}$ ) for maize (a,b), barley (c,d) and the olive crop (e,f).

The statistical indicators relative to the comparison between  $K_{cb\ VI}$  and  $K_{cb\ SIMDualKc}$  for all crops are presented in Table 5. The RMSD between  $K_{cb\ VI}$  and  $K_{cb\ SIMDualKc}$  for the set of image dates considered for maize was equal to 0.16 when using NDVI for the computation of  $K_{cb\ VI}$  and 0.22 when SAVI was adopted. RMD was also higher when adopting SAVI. The regression coefficient  $b = 0.98$  when NDVI is used indicates a statistical similarity between  $K_{cb\ VI}$  and  $K_{cb\ field}$ . For barley,  $b$  and  $R^2$  are higher for  $K_{cb\ NDVI}$  and RMSD and RMD are smaller than for  $K_{cb\ SAVI}$ . For the olive crop there is a clear

overestimation of  $K_{cb\ NDVI}$  and  $K_{cb\ SAVI}$  when the  $f_c\ VI$  is computed with NDVI (1.81 and 1.19, respectively; Table 5).

**Table 5.** Statistical indicators relative to the comparison between  $K_{cb\ VI}$  and  $K_{cb\ SIMDualKc}$  for maize and barley when  $f_c\ VI$  computed with NDVI and for olive crops when  $f_c\ VI$  is computed with NDVI and SAVI \*.

		b	R <sup>2</sup>	n	p	Estimation		Cross Validation	
						RMSD ( )	RMD (%)	RMSD ( )	RMD (%)
Maize	$K_{cb\ NDVI}$	0.98	0.74	15	0.0000389	0.16	14.8	0.08	8.4
	$K_{cb\ SAVI}$	0.79	0.79	15	0.0000094	0.22	21.1	0.18	20.9
Barley	$K_{cb\ NDVI}$	0.99	0.95	7	0.0001935	0.07	9.6	0.04	4.7
	$K_{cb\ SAVI}$	0.67	0.89	7	0.0014203	0.23	32.0	0.22	31.3
Olive	$K_{cb\ NDVI}$	1.81	0.56	15	0.0013317	0.31	81.1	0.30	82.5
	$K_{cb\ SAVI}$	1.19	0.72	15	0.0000023	0.08	21.7	0.07	19.0
	$K_{cb\ SAVI\ *}$	1.03	0.88	15	0.0000002	0.02	5.6	0.01	3.3

\*  $f_c$  estimated from SAVI.

For the olive crop, however, estimating  $K_{cb\ VI}$  using  $f_c\ SAVI$  (see Equations (6) and (7)) provided much better results (Figure 5 and Table 5;  $K_{cb\ SAVI\ *}$ ) than using  $K_{cb\ VI}$  with  $f_c\ NDVI$  (Table 5). Comparing  $K_{cb\ SAVI}$  with  $K_{cb\ SIMDualKc}$  it results a higher  $R^2 = 0.88$  with b of 1.03 (Table 5). In addition, RMSD decreased from 0.08 to 0.02 and RMD from 21.7 to 5.6% (Table 5). RMSD and RMD obtained in the cross validation procedure for the three crops are also presented in Table 5. The results obtained for cross validation are consistent with those obtained for the estimation procedure.

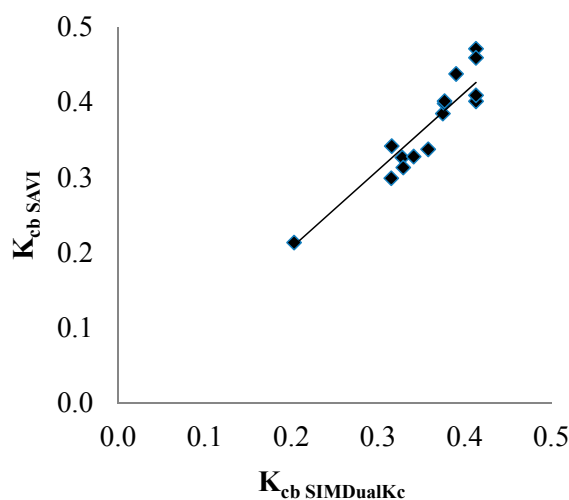


**Figure 5.** Comparison of actual  $K_{cb}$  obtained with SIMDualKc ( $K_{cb\ SIMDualKc}$ ) with  $K_{cb}$  derived from SAVI ( $K_{cb\ SAVI}$ ) for olive when  $f_c$  is estimated from SAVI.

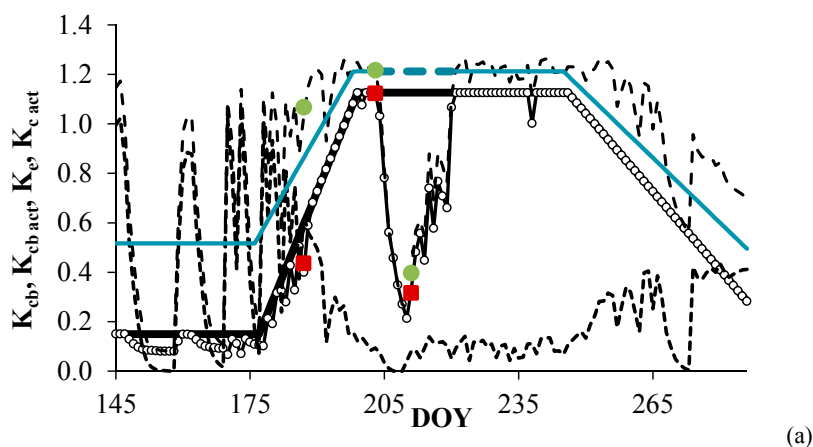
Table 6 presents the average and standard error of the mean or the range of the  $K_{cb\ VI}$  obtained for all fields and all crops. Results refer to the use of both NDVI and SAVI with Equation (6). As for the previous analysis, the best results refer to  $K_{cb\ NDVI}$  in case of maize and barley and  $K_{cb\ SAVI}$  in case of the olive orchard. Comparing results for both VIs in this Table 6 it becomes apparent that estimations using NDVI lead to higher  $K_{cb\ VI}$  results, which relates to the nature of the VI index.

**Table 6.** Average and standard error of the mean or the range of the actual daily basal crop coefficients estimated with vegetation indices for the various crops and crop growth stages.

Crop Growth Stages	Maize	Barley	Olive
$K_{cb,NDVI}$			
Initial	(1)	<b>0.18</b> ( ) <sup>(2)</sup>	0.78 ( $\pm 0.13$ )
Development <sup>(4)</sup>	<b>[0.44–1.00]</b>	<b>[0.25–0.91]</b>	[0.53–0.77] <sup>(3)</sup>
Mid-season	<b>0.92 (<math>\pm 0.11</math>)</b> <sup>(5)</sup>	<b>0.87</b> ( ) <sup>(2)</sup>	0.61 ( $\pm 0.05$ ) <sup>(6)</sup>
Late-season <sup>(4)</sup>	<b>[0.84–0.46]</b>	<b>[0.86–0.69]</b>	[0.75–0.55]
$K_{cb,SAVI}$			
Initial	(1)	0.15 ( ) <sup>(2)</sup>	<b>0.33 (<math>\pm 0.01</math>)</b>
Development <sup>(4)</sup>	[0.33–0.76]	[0.20–0.63]	<b>[0.30–0.44]</b> <sup>(3)</sup>
Mid-season	0.76 ( $\pm 0.10$ ) <sup>(5)</sup>	0.54 ( ) <sup>(2)</sup>	<b>0.37 (<math>\pm 0.03</math>)</b> <sup>(6)</sup>
Late-season <sup>(4)</sup>	[0.52–0.33]	[0.56–0.52]	<b>[0.40–0.33]</b>

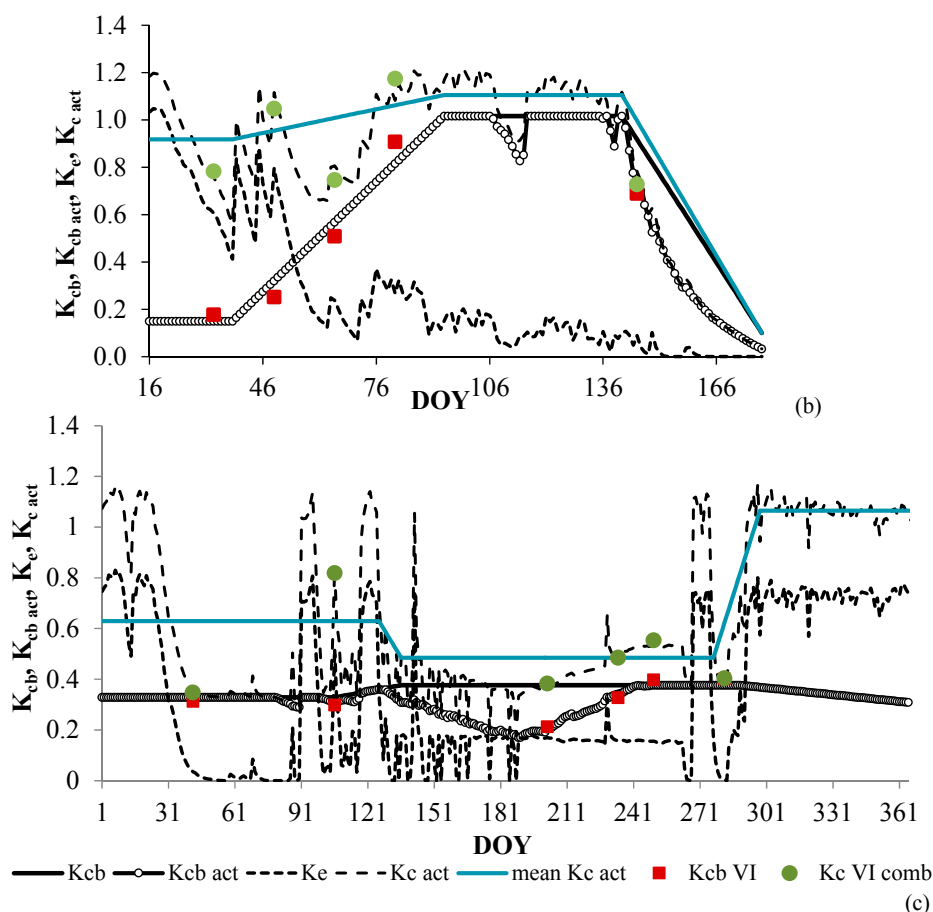
Note:  $f_{c,VI}$  were obtained from NDVI for maize and barley and from SAVI for olive. <sup>(1)</sup> No Landsat images available for this crop growth stage; <sup>(2)</sup> Only one Landsat image available for this crop growth stage; <sup>(3)</sup> Period after pruning; <sup>(4)</sup> Range of values for this crop growth stage; <sup>(5)</sup> Stress occurred in three out of the eight image dates considered; <sup>(6)</sup> Stress occurred in four out of the eight image dates considered.

Figure 6 shows selected examples of the seasonal variation of the daily  $K_{cb}$ ,  $K_{cb,act}$ ,  $K_e$  and  $K_c$  act obtained with SIMDualKc for maize [34], barley [35] and olive [8] and the fitting of actual  $K_{cb,VI}$  obtained for those sets of data.  $K_{cb,VI}$  used in Figure 6 refer to  $K_{cb,NDVI}$  in case of maize and barley and to  $K_{cb,SAVI}$  in case of olive. For the olive orchard, the  $f_{c,SAVI}$  (Equation (7)) were used in the computation of  $K_d$  while  $f_{c,NDVI}$  were used for maize and barley. Unfortunately, there were few images for maize crop in the year when water stress occurred. Results show that actual  $K_{cb,VI}$  match quite well the actual  $K_{cb}$  curve for the three crops. The variability of weather conditions in those years are well apparent through the numerous peaks of the evaporation coefficient  $K_e$  due to both rainfall and irrigation events. The effect of water stress on  $K_{cb}$  is well apparent by the deviations of  $K_{cb,act}$  from the potential  $K_{cb}$ , thus when the  $K_{cb,act}$  curve lays below the  $K_{cb}$  curve. Summarizing, Figure 6 demonstrates the goodness of the approach used to estimate  $K_{cb,act}$  from a vegetation index.



**Figure 6.** Cont.





**Figure 6.** Seasonal variation of the daily coefficients  $K_{cb}$ , actual  $K_{cb}$  ( $K_{cb\ act}$ ),  $K_e$  and actual  $K_c$  ( $K_{c\ act}$ ) obtained with SIMDualKc, and actual  $K_{cb\ VI}$  and actual  $K_c$  estimated by the combined approach ( $K_{c\ VI}$ ) for: (a) maize, field 1—Year 2010; (b) barley, year 2012; and (c) olive orchard, year 2012.

### 3.3. Estimation of Actual $K_c$ from Reflectance-Based Vegetation Indices ( $K_{c\ VI}$ )

The actual  $K_{c\ VI}$  values were obtained by combining the actual  $K_{cb\ VI}$  with  $K_e$  derived from SIMDualKc. The results for  $K_{c\ VI}$  presented in Figure 7 and Table 7 were obtained using the  $K_{cb\ VI}$  that provided the best estimation for each crop as presented in Section 3.2. Thus,  $K_{cb\ NDVI}$  was considered for the computation of  $K_{c\ VI}$  for maize and barley crops, while  $K_{cb\ SAVI}$  was adopted for olive. Figure 6 shows the  $K_{c\ VI}$  corresponding to the same dates when the  $K_{cb\ VI}$  were obtained for selected data sets referred in Section 3.2. It may be observed that despite the enormous variability of  $K_e$  due to rainfall and irrigation wetting events the computed  $K_{c\ VI}$  match well the actual  $K_c$  curves for the three crops analyzed.

**Table 7.** Statistical indicators relative to the comparison between actual  $K_{c\ VI}$  and  $K_{c\ SIMDualKc}$ .

b	$R^2$	n	p	Estimation		Cross Validation		
				RMSD ( )	RMD (%)	RMSD ( )	RMD (%)	
Maize	0.99	0.72	15	0.0000637	0.16	12.7	0.08	6.9
Barley	0.99	0.83	7	0.0043194	0.07	6.4	0.03	2.6
Olive	1.01	0.99	15	0.0000000	0.02	3.3	0.01	2.1

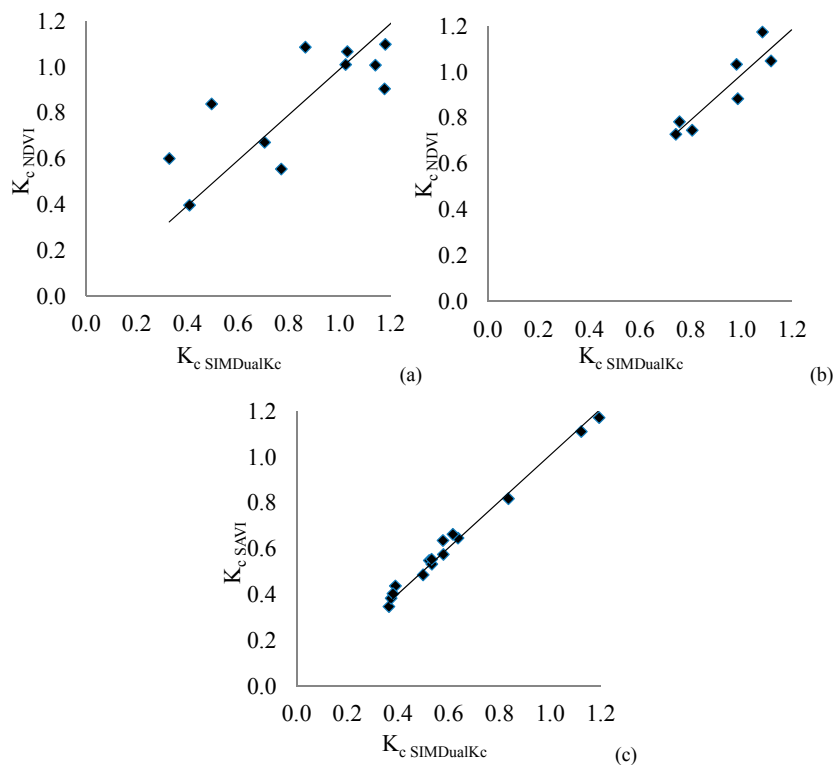


**Figure 7.** Comparison of actual  $K_c$  derived from SIMDualKc ( $K_{c \text{ SIMDualKc}}$ ) and actual  $K_c$  derived from the combined approach of  $K_{cb \text{ VI}}$  and  $K_e$  from SIMDualKc ( $K_{c \text{ VI}}$ ) for (a) maize; (b) barley; and (c) olive.

When comparing  $K_{c \text{ VI}}$  and  $K_{c \text{ SIMDualKc}}$  a high determination coefficient was obtained ( $R^2 \geq 0.72$ ) together with a regression coefficient very close to 1.0 for the three crops studied (Figure 7 and Table 7). The best statistical indicators were obtained for the olive orchard (Table 7), particularly with quite small RMSD and RMS. RMSD and RMD obtained in the cross validation procedure for the three crops show results very similar to those obtained for the estimation procedure (Table 7).

The average and range of the actual crop coefficients estimated with vegetation indices combined with the computed  $K_e$  ( $K_{c \text{ VI}}$ ) are given in Table 8 for the various crops.

**Table 8.** Average and standard error of the mean or the range of actual crop coefficients estimated with vegetation indices approach ( $K_{c \text{ VI}}$ ) for the various crop growth stages of each crop.

Crop Growth Stages	Maize	Barley	Olive
Initial	(1)	0.78 ( ) (2)	0.76 ( $\pm 0.41$ ) (3)
Development (4)	[0.90–1.30] (5)	[0.75–1.18]	[0.44–0.82] (6)
Mid-season	0.98 ( $\pm 0.11$ ) (7)	0.88 ( ) (2)	0.62 ( $\pm 0.08$ ) (8)
Late-season (4)	[0.84–0.55]	[1.03–0.73]	[0.53–0.40]

Note:  $f_{c \text{ VI}}$  were obtained from NDVI for maize and barley and from SAVI for olive. (1) No Landsat images available for this crop growth stage; (2) Only one Landsat image available for this crop growth stage; (3) High evaporation occurrence in one of the image dates considered in the initial stage due to precipitation occurrence. (4) Range of daily  $K_c$  values (not time-averaged); (5) High evaporation in two of the dates considered in this crop growth stage; (6) Period after pruning; (7) Stress occurred in three out of the eight image dates considered; (8) Stress occurred in four out of the eight image dates considered.

## 4. Discussion

### 4.1. Estimation of the Fraction of Ground Cover from Vegetation Indices

The statistical results relative to the estimation of  $f_c$   $_{VI}$  indicate a good performance of Equation (7) for the annual crops studied (maize and barley). The  $R^2$  values observed when comparing  $f_c$   $_{VI}$  with  $f_c$   $_{field}$  are highly significant for both crops (Figure 3). These  $R^2$  values are within the range of the values reported by Trout *et al.* [56] for the estimation of canopy cover using NDVI derived from a multispectral camera for a set of 11 annual and perennial horticultural crops. Purevdorj *et al.* [57] reported similar  $R^2$  results when estimating the percentage of vegetation cover in grasslands and lawn grass using NDVI derived from AVHRR satellite images, thus with a coarser spatial resolution. Estimated deviations are small, for both maize and barley, with RMSD of 0.10 and 0.06, respectively.

The estimation of  $f_c$  in the olive orchard also showed good estimation, with low RMD < 10%. When the two years studied (2011 and 2012) were analyzed separately, the average absolute deviations between  $f_c$   $_{VI}$  and  $f_c$   $_{field}$  were slightly higher in 2012 than in 2011. These results are likely due to the larger variability in the vegetation conditions within the orchard in 2012 because a severe frost occurred in February which was followed by an heavy and non-uniform pruning that increased the variability of  $f_c$  within the orchard as discussed by Paço *et al.* [8].

The better performance of SAVI for the estimation of  $f_c$   $_{VI}$  in the high density olive orchard, having a large fraction of soil exposed, is likely due to the lower sensitivity of this VI to soil background influence [23]. Similar conclusions were reported by Purevdorj *et al.* [57] relative to the better performance of SAVI to estimate the vegetation cover for low crop densities. Differently, in a study with savannah-type open woodlands dominated by evergreen oak species (*montados* or *dehesa*), the NDVI performed slightly better than SAVI for the estimation of tree canopy cover [58] but the study areas were characterized by an extremely variable understory including bare soil, dry grass and a few evergreen shrubs that impacted the VIs values as discussed by the authors.

### 4.2. Estimation of Actual $K_{cb}$ from Reflectance-Based Vegetation Indices ( $K_{cb}$ $_{VI}$ )

The  $R^2$  results relative to the regression comparing the actual  $K_{cb}$   $_{VI}$  with  $K_{cb}$   $_{SIMDualKc}$  for maize were highly significant using NDVI (Table 5). Although using NDVI led to a lower  $R^2$  than SAVI, the regression coefficient comparing  $K_{cb}$   $_{SAVI}$  with  $K_{cb}$   $_{SIMDualKc}$  ( $b = 0.79$ ; Table 5) indicates an underestimation of  $K_{cb}$   $_{SAVI}$  values. The regression coefficient obtained when comparing  $K_{cb}$   $_{NDVI}$  with  $K_{cb}$   $_{SIMDualKc}$  is much better ( $b = 0.98$ ; Table 5), which may be related with the tendency of NDVI reaching a maximum value at about the same time as  $K_{cb}$ , *i.e.*, at a LAI around 3 [14,59]. Contrarily, SAVI tends to continue increasing for LAI above 3 [21,25,60]. Thus, according to Allen *et al.* [21], the NDVI supports better than SAVI the estimation of  $K_c$  and  $K_{cb}$  in crops reaching high LAI values as for the full cover crops considered in the current study.

The base data on maize refers to three different seasons and three different fields, which results in a large variability of soil, climate and crop management conditions. A large variability of  $K_{cb}$   $_{act}$  was therefore observed despite the potential/standard  $K_{cb}$  was the same after appropriate calibration of  $SIMDualKc$  [34]. This variability contributed for a larger variance of the actual  $K_{cb}$   $_{VI}$  and  $K_{cb}$   $_{SIMDualKc}$  and made it more difficult to parameterize a single value for  $K_c$   $_{min}$  and  $\beta_1$  (Equations (6) and (7),

respectively) when considering all three maize seasons and three cropped fields. The variability conditions observed in the three different fields and seasons during the initial and development stages may justify why comparing  $K_{cb\ NDVI}$  with  $K_{cb\ SIMDualKc}$  leads to a smaller  $R^2$  (Table 5).

The actual  $K_{cb\ NDVI}$  obtained for the maize mid-season stage averaged 0.92 (Table 6). This value relates with the water stress that occurred during the mid-season stage of 2010 in both surveyed fields which was detected in two of the images, particularly that of 30 July 2010. The SIMDualKc computed  $K_s$  values for this date were 0.55 and 0.29 respectively for field 1 and field 2. Such low  $K_s$  values highly impacted actual  $K_{cb}$  for this stage. Figure 6a shows well the impact of water stress during that period, with the  $K_{cb\ act}$  curve largely below the  $K_{cb}$  curve. The actual  $K_{cb\ NDVI}$  are within the range of values presented by Padilla *et al.* [31]. Relative to the late season, the range of  $K_{cb\ NDVI}$  values in Table 6 refer to three images available for this period. One of these images was captured the day prior to harvest (19 September 2011 in field 1) and the  $K_{cb\ NDVI}$  was then equal to 0.48, therefore similar to the  $K_{cb\ end}$  proposed by Allen *et al.* [1],  $K_{cb\ end} = 0.5$ . However, values for  $K_{cb\ end}$  relate to crop management and therefore are difficult to be compared with other values in literature.

For the regression comparing the actual  $K_{cb\ VI}$  and  $K_{cb\ SIMDualKc}$  for barley the statistical indicators show that NDVI performed better, both in terms of the regression and determination coefficients and RMSD and RMD (Table 5 and Figure 4c,d). The actual  $K_{cb\ NDVI}$  obtained for the initial crop growth stage (actual  $K_{cb\ ini\ NDVI} = 0.18$ ; Table 6) is just slightly higher than the value presented by Allen *et al.* [1],  $K_{cb\ ini} = 0.15$ , which relates with the fact that no water stress occurred in that stage (Figure 6b).  $K_{cb\ NDVI}$  values for the development growth stage ranged between 0.25 and 0.91 (Table 6), which refer to values commonly accepted [1]. The actual  $K_{cb\ mid\ NDVI} = 0.87$  (Table 6) is lower than the standard  $K_{cb} = 1.10$  proposed by Allen *et al.* [1] and values obtained for crops with similar canopy [30,31,61]. This is likely due to different vegetation conditions in the 2012/2013 crop season and to the adjustment to climate [35]. The  $K_{cb\ NDVI}$  presented in Table 6 for the late season ranged between 0.86 and 0.69 and refer to two images available for that stage. These images provided for likely appropriate actual  $K_{cb}$  values and compared well with values obtained with SIMDualKc (Figure 6b, [35]).

For the olive orchard, results obtained with SAVI are good (Figure 5) and in agreement with the above mentioned lower sensitivity of this VI to changes in soil background [23], which is particularly relevant for tree crops with discontinuous ground cover. Furthermore, SAVI improves the linearity between the VI and biophysical parameters as observed by other researchers [25,56]. Mateos *et al.* [7] also obtained good results when using SAVI for estimating  $K_{cb}$  in peach and mandarin orchards. Contrarily, in a study with grapevine, Campos *et al.* [13] did not find significant improvements in the accuracy when using SAVI but the application excluded days with wet soil. Accurate results for olive in the current study are likely due to the use of  $K_d$  in Equation (6).

The average  $K_{cb\ SAVI}$  value obtained for the mid-season stage in olive (0.37; Table 6 and Figure 5c) was affected by the occurrence of water stress in four out of the eight dates considered in this stage, with  $K_s < 0.77$  in two of these dates. The impacts of water stress on  $K_{cb}$  is clearly shown in the example presented in Figure 6c, with the  $K_{cb\ act}$  curve laying bellow the  $K_{cb}$  curve during the mid-season. The actual  $K_{cb\ SAVI}$  for this stage would increase to 0.42 when only dates without water stress or with very mild stress ( $K_s > 0.95$ ) are considered. The actual  $K_{cb\ SAVI}$  values for olive orchards for the mid- and late-seasons, respectively 0.37 and ranging 0.40 to 0.33 (Table 6), are within the range of values for olive orchards with an effective fraction of ground cover ( $f_{c\ eff}$ ) between 0.25 and 0.5,

with a  $K_{cb\ mid}$  ranging between 0.35 and 0.55 and  $K_{cb\ end}$  ranging from 0.30 to 0.50 [12]. During the initial stage, some sparse vegetation was growing in the inter-rows, thus  $K_{cb}$  was only slightly influenced by this sparse vegetation. Consequently,  $K_{cb\ ini\ SAVI} = 0.33$  was an appropriate value for this orchard.

Overall results obtained have shown a good performance of the  $K_{cb\ VI}$  Equation (6) for all three crops, particularly integrating results of  $f_c\ VI$  when computing the density coefficient  $K_d$  used in Equation (6). It must be stressed that the use of  $K_d$ , which integrates the information on  $f_c$  and crop height, and of  $K_{c\ min}$  provided good results in modeling the actual  $K_{cb\ VI}$  (Equation (6)) for crops with very different canopy structures and ground cover conditions as those used in this study (continuous *versus* discontinuous ground cover) for the whole crop season including when water stress was observed.

#### 4.3. Estimation of Actual $K_c$ by Combining $K_{cb\ VI}$ with $K_e$ from SIMDualKc ( $K_c\ VI$ )

The statistical indicators from comparing the actual  $K_{c\ VI}$  with  $K_{c\ SIMDualKc}$  show a good performance of the model for the three crops (Table 7 and Figure 7). The deviations of estimate are very low for olive and barley and slightly higher for maize. Results are in agreement with those discussed for  $K_{cb\ VI}$ , which is a component of  $K_{c\ VI}$ .

For the maize crop, the actual  $K_{c\ NDVI}$  values obtained for the development stage ranged between 0.90 and 1.30, which relate with a large variability of  $K_e$  values, as for the example in Figure 6a. The average  $K_{c\ NDVI} = 0.98 \pm 0.11$  for the mid-season (Table 8) reflects also a large variability as exemplified in Figure 6a, where one value exceeds 1.20 and the other, due to water stress, is as low as 0.40. When only cases without water stress are considered,  $K_{c\ VI}$  increases to 1.14, a value close to the  $K_c$  reported by Gonzalez-Piqueras *et al.* [26]. Regarding the  $K_{c\ NDVI}$  values for the late-season, values obtained are likely to occur because they are within the interval limited by the  $K_c$  values at mid-season and those expected for end season.

The actual  $K_{c\ NDVI}$  estimated for the initial and development stages for barley (0.78 and 0.75–1.18; Table 8) reflects the abundance of rainfall during these stages, with various  $K_e$  peaks occurring then (Figure 6b). For the mid-season stage the value obtained is lower than the values estimated with SIMDualKc ( $K_{c\ SIMDualKc} = 0.99$ ), thus indicating an underestimation of  $K_c$ . The average value obtained for the late-season stage (0.88) is close to that obtained by Liu *et al.* [62] for the period between wax ripeness and harvesting (equal to 0.83).

The results obtained for the olive orchard show a very good performance of the model for estimating  $K_{c\ SAVI}$  (Figure 7c). The average results of  $K_{c\ SAVI}$  (Table 8) are within the range of those proposed by Allen and Pereira [12] for an  $f_{c\ eff}$  between 0.25 and 0.50, which vary between 0.80 for the  $K_{c\ ini}$  (considering an active ground cover), 0.40–0.60 for the  $K_{c\ mid}$  (no active ground cover), and 0.35–0.75 for the  $K_{c\ end}$  (depending on the ground cover). The results obtained throughout the year follow a pattern similar to results reported by other authors [43,63], as discussed by Paço *et al.* [8].

It is important to highlight that results presented herein correspond to actual  $K_c$ , thus reflecting the management options observed in the study areas.

## 5. Conclusions

The overall results for the three crops—Maize, barley and olive—indicate that the newly proposed Equation (7) adequately models the fraction of soil covered by vegetation throughout the crop season. The results obtained indicate a better performance of SAVI for the computation of the fraction of ground cover for the incomplete cover crop, olive, and of the NDVI for the annual crops, maize and barley.

Using the novel Equation (6), which applies a density coefficient, the estimation of actual basal crop coefficients through reflectance-based vegetation indices was successful, with good accuracy. The use of NDVI was preferred for maize and barley and SAVI was more accurate for olive. These results are consistent with the lower sensitivity of SAVI to changes of reflectance in soil background due to soil moisture. This approach allowed considering the whole crop season, including periods when the soil cover by vegetation is low, as in the initial and development growth stages, which was not considered in several studies previously published in the literature. The use of the density coefficient allowed considering crops with different canopy structures and incorporating the impact of vegetation density and height. The use of the stress coefficient computed with the soil water balance SIMDualKc made it possible to apply the methodology not only in days when soil water was adequate to sustain full plant transpiration but also in days when heavy water stress conditions occurred, contrarily to most of the approaches previously published that do not account for the crop water stress in their formulation.

The proposed methodology for estimating actual crop coefficients follows a dual crop coefficient approach by combining a remotely sensed basal crop coefficient and an evaporation coefficient computed with the soil water balance SIMDualKc. Therefore, the approach allows integrating the effect of plant transpiration with that of soil evaporation.

The approaches proposed in this study, combining VI data with soil water balance data, provide for an operational methodology to support irrigation management considering the actual cropping conditions and associating real time satellite information with irrigation scheduling models potentially applicable to diverse crop types. Nevertheless, further studies are desirable to better test and implement the methodology, particularly for other crops and using a larger number of image dates.

## Acknowledgments

This study was supported by European Union Funds (FEDER/COMPETE—Operational Competitiveness Program) and by national funds (FCT—Portuguese Foundation for Science and Technology) under the project EXPL/AGRO-PRO/1559/2012 and the project AGR-PRO/111717/2009. The first author acknowledges the FCT—Portuguese Foundation for Science and Technology for the Post-Doc research grant (SFRH/BPD/79767/2011).

## Author Contributions

The first author contributed for the current study by processing the satellite imagery, including the calibration of the images and the computation of vegetation indices, developing and testing the newly proposed methodology in combination with the other authors, and assuming the responsibility of

writing the present manuscript, also in collaboration with the other authors. The second and third authors contributed with field work and SIMDualKc modeling relative to the crops studied as well as contributing to test the approaches. The fourth author was responsible for the remote sensing study while the fifth and senior author was responsible for aspects related with evapotranspiration and water balance and for the revision of the manuscript.

### List of Symbols and Acronyms

$D_r$	Root zone depletion [mm]
ET	Evapotranspiration [mm]
$ET_c$	Crop evapotranspiration [mm]
$ET_o$	Reference evapotranspiration [mm]
$f_c$	Fraction of ground cover [ ]
$f_{c \text{ field}}$	Fraction of ground cover based on field data [ ]
$f_{c \text{ VI}}$	Fraction of ground cover based on vegetation indices data [ ]
$f_{ew}$	Fraction of the soil that is both exposed and wetted [ ]
$f_{c \text{ eff}}$	Effective fraction of ground covered or shaded by vegetation near solar noon [ ]
$h$	Mean height of the vegetation [m]
$K_c$	Crop coefficient [ ]
$K_{c \text{ act}}$	Actual crop coefficient [ ]
$K_{cb \text{ act}}$	Actual basal crop coefficient [ ]
$K_{cb \text{ cover}}$	$K_{cb}$ of the ground cover in the absence of tree foliage [ ]
$K_{cb \text{ full}}$	Estimated basal $K_{cb}$ for peak plant growth conditions having nearly full ground cover [ ]
$K_{c \text{ max}}$	Maximum value of $K_c$ following rain or an irrigation event [ ]
$K_{c \text{ min}}$	Minimum $K_c$ for bare soil [ ]
$K_{c \text{ VI}}$	$K_{c \text{ act}}$ computed combining the $K_{cb \text{ act}}$ derived from vegetation indices and the $K_e$ derived from SIMDualKc [ ]
$K_{c \text{ NDVI}}$	$K_{c \text{ act}}$ computed combining the $K_{cb \text{ act}}$ derived from NDVI and the $K_e$ derived from SIMDualKc [ ]
$K_{c \text{ SAVI}}$	$K_{c \text{ act}}$ computed combining the $K_{cb \text{ act}}$ derived from SAVI and the $K_e$ derived from SIMDualKc [ ]
$K_{c \text{ SIMDualKc}}$	$K_c$ computed with SIMDualKc [ ]
$K_{cb \text{ VI}}$	$K_{cb \text{ act}}$ computed from a vegetation index [ ]
$K_{cb \text{ NDVI}}$	$K_{cb \text{ act}}$ computed from NDVI [ ]
$K_{cb \text{ SAVI}}$	$K_{cb \text{ act}}$ computed from SAVI [ ]
$K_{cb \text{ SIMDualKc}}$	$K_{cb \text{ act}}$ computed with SIMDualKc [ ]
$K_d$	Density coefficient [ ]
$K_e$	Soil evaporation coefficient [ ]
$K_r$	Evaporation reduction coefficient dependent on the cumulative depth of water depleted (evaporated) from the topsoil [ ]
$K_s$	Water stress coefficient [ ]

LAI	Leaf area index [ $\text{m}^2 \cdot \text{m}^{-2}$ ]
$M_L$	Multiplier on $f_{c \text{ eff}}$ describing the effect of canopy density on shading and on maximum relative ET per fraction of ground shaded [ ]
$p$	Soil water depletion fraction for no stress [ ]
TAW	Total available water [mm]
RAW	Readily available soil water [mm]
RMD	Relative mean difference [%]
RMSD	Root-mean-square deviation [ ]
a.s.l.	Above sea level [m]
ETM+	Enhanced thematic mapper
NDVI	Normalized difference vegetation index
NIR	Near infrared
RS	Remote sensing
SAVI	Soil adjusted vegetation index
TM	Thematic mapper
VI	Vegetation index
$VI_i$	VI for a specific date and pixel
$VI_{\text{max}}$	VI for maximum vegetation cover
$VI_{\text{min}}$	VI for minimum vegetation cover
$\beta_1$	Empirical coefficient depending upon the maximum NDVI value in each crop growth stage
$\beta_2$	Adjustment coefficient associated with crop senescence and leaves yellowing

## Conflicts of Interest

The authors declare no conflict of interest.

## References

- Allen, R.G.; Pereira, L.S.; Raes, D.; Smith, M. *Crop Evapotranspiration: Guidelines for Computing Crop Water Requirements*. *FAO Irrigation and Drainage Paper 56*; FAO—Food and Agriculture Organization of the United Nations: Rome, Italy, 1998; p. 300.
- Monteith, J.L. Evaporation and environment. In *19th Symposia of the Society for Experimental Biology*; University Press: Cambridge, CA, USA, 1965; pp. 205–234.
- Shuttleworth, W.J.; Wallace, J.S. Calculating the water requirements of irrigated crops in Australia using the Matt-Shuttleworth approach. *Trans. ASABE* **2009**, *52*, 1895–1906.
- Bastiaanssen, W.G.M.; Noordman, E.J.M.; Pelgrum, H.; Davids, G.; Thoreson, B.P.; Allen, R.G. SEBAL model with remotely sensed data to improve water-resources management under actual field conditions. *J. Irrig. Drain. Eng.* **2005**, *131*, 85–93.
- Allen, R.G.; Tasumi, M.; Trezza, R. Satellite-based energy balance for mapping evapotranspiration with internalized calibration (METRIC)—Model. *J. Irrig. Drain. Eng.* **2007**, *133*, 380–394.



6. Kustas, W.P.; Norman, J.M.; Schmugge, T.J.; Anderson, M.C. Mapping surface energy fluxes with radiometric temperature. Chapter 7. In *Thermal Remote Sensing in Land Surface Processes*; Quattrochi, D., Luvall, J., Eds.; CRC Press: Boca Raton, FL, USA, 2004; pp. 205–253.
7. Mateos, L.; González-Dugo, M.P.; Testi, L.; Villalobos, F.J. Monitoring evapotranspiration of irrigated crops using crop coefficients derived from time series of satellite images. I. Method validation. *Agric. Water Manag.* **2013**, *125*, 81–91.
8. Paço, T.A.; Pôças, I.; Cunha, M.; Silvestre, J.C.; Santos, F.L.; Paredes, P.; Pereira, L.S. Evapotranspiration and crop coefficients for a super intensive olive orchard. An application of SIMDualKc and METRIC models using ground and satellite observations. *J. Hydrol.* **2014**, *519B*, 2067–2080.
9. Pakparvar, M.; Cornelis, W.; Pereira, L.S.; Gabriels, D.; Hosseinimarandi, H.; Edraki, M.; Kowsar, S.A. Remote sensing estimation of actual evapotranspiration and crop coefficients for a multiple land use arid landscape of southern Iran with limited available data. *J. Hydroinf.* **2014**, *16*, 1441–1460.
10. Pôças, I.; Cunha, M.; Pereira, L.S.; Allen, R.G. Using remote sensing energy balance and evapotranspiration to characterize montane landscape vegetation with focus on grass and pasture lands. *Int. J. Appl. Earth Obs. Geoinf.* **2013**, *21*, 159–172.
11. Pereira, L.S.; Allen, R.G.; Smith, M.; Raes, D. Crop evapotranspiration estimation with FAO56: Past and future. *Agric. Water Manag.* **2015**, *147*, 4–20.
12. Allen, R.G.; Pereira, L.S. Estimating crop coefficients from fraction of ground cover and height. *Irrig. Sci.* **2009**, *28*, 17–34.
13. Campos, I.; Neale, C.M.U.; Calera, A.; Balbontín, C.; González-Piqueras, J. Assessing satellite-based basal crop coefficients for irrigated grapes (*Vitis vinifera* L.). *Agric. Water Manag.* **2010**, *98*, 45–54.
14. Calera, A.; Jochum, A.M.; García, A.C.; Rodríguez, A.M.; Fuster, P.L. Irrigation management from space: Towards user-friendly products. *Irrig. Drain. Syst.* **2005**, *19*, 337–353.
15. Allen, R.G.; Tasumi, M.; Morse, A.; Trezza, R.; Wright, J.L.; Bastiaanssen, W.; Kramber, W.; Lorite, I.; Robison, C.W. Satellite-based energy balance for mapping evapotranspiration with internalized calibration (METRIC)—Applications. *J. Irrig. Drain. Eng.* **2007**, *133*, 395–406.
16. Glenn, E.P.; Huete, A.R.; Nagler, P.L.; Nelson, S.G. Relationship between remotely-sensed vegetation indices, canopy attributes and plant physiological processes: What vegetation indices can and cannot tell us about the landscape. *Sensors* **2008**, *8*, 2136–2160.
17. Glenn, E.P.; Neale, C.M.U.; Hunsaker, D.J.; Nagler, P.L. Vegetation index-based crop coefficients to estimate evapotranspiration by remote sensing in agricultural and natural ecosystems. *Hydrol. Process.* **2011**, *25*, 4050–4062.
18. Johnson, L.F.; Trout, T.J. Satellite NDVI assisted monitoring of vegetable crop evapotranspiration in California’s San Joaquin valley. *Remote Sens.* **2012**, *4*, 439–455.
19. Viña, A.; Gitelson, A.A.; Nguy-Robertson, A.L.; Peng, Y. Comparison of different vegetation indices for the remote assessment of green leaf area index of crops. *Remote Sens. Environ.* **2011**, *115*, 3468–3478.
20. Hunsaker, D.; Pinter, P.J., Jr.; Kimball, B. Wheat basal crop coefficients determined by normalized difference vegetation index. *Irrig. Sci.* **2005**, *24*, 1–14.

21. Allen, R.G.; Pereira, L.S.; Howell, T.A.; Jensen, M.E. Evapotranspiration information reporting: I. Factors governing measurement accuracy. *Agric. Water Manag.* **2011**, *98*, 899–920.
22. Rouse, W.; Haas, R.; Scheel, J.; Deering, W. Monitoring Vegetation Systems in Great Plains with ERTS. In Proceedings of the Third ERTS Symposium, NASA SP-351, Washington, DC, USA, 10–14 December 1973; US Government Printing Office: Washington, DC, USA, 1973; pp. 309–317.
23. Huete, A.R. A soil-adjusted vegetation index (SAVI). *Remote Sens. Environ.* **1988**, *25*, 295–309.
24. Jensen, J.R. *Remote Sensing of Environment. An Earth Resource Perspective*; Prentice Hall, Inc.: Upper Saddle River, NJ, USA, 2000.
25. Choudhury, B.J.; Ahmed, N.U.; Idso, S.B.; Reginato, R.J.; Daughtry, C.S.T. Relations between evaporation coefficients and vegetation indices studied by model simulations. *Remote Sens. Environ.* **1994**, *50*, 1–17.
26. Jayanthi, H.; Neale, C.M.U.; Wright, J.L. Development and validation of canopy reflectance-based crop coefficient for potato. *Agric. Water Manag.* **2007**, *88*, 235–246.
27. Hunsaker, D.J.; Pinter, P.J., Jr.; Barnes, E.M.; Kimball, B.A. Estimating cotton evapotranspiration crop coefficients with a multispectral vegetation index. *Irrig. Sci.* **2003**, *22*, 95–104.
28. Bausch, W.C.; Neale, C.M.U. Crop coefficients derived from reflected canopy radiation: A concept. *Trans. ASAE* **1987**, *30*, 703–709.
29. Er-Raki, S.; Rodriguez, J.C.; Garatuza-Payan, J.; Watts, C.J.; Chehbouni, A. Determination of crop evapotranspiration of table grapes in a semi-arid region of Northwest Mexico using multi-spectral vegetation index. *Agric. Water Manag.* **2013**, *122*, 12–19.
30. Er-Raki, S.; Chehbouni, A.; Guemouria, N.; Duchemin, B.; Ezzahar, J.; Hadria, R. Combining FAO-56 model and ground-based remote sensing to estimate water consumptions of wheat crops in a semi-arid region. *Agric. Water Manag.* **2007**, *87*, 41–54.
31. Padilla, F.L.M.; González-Dugo, M.P.; Gavilán, P.; Domínguez, J. Integration of vegetation indices into a water balance model to estimate evapotranspiration of wheat and corn. *Hydrol. Earth Syst. Sci.* **2011**, *15*, 1213–1225.
32. Rosa, R.D.; Paredes, P.; Rodrigues, G.C.; Alves, I.; Fernando, R.M.; Pereira, L.S.; Allen, R.G. Implementing the dual crop coefficient approach in interactive software. 1. Background and computational strategy. *Agric. Water Manag.* **2012**, *103*, 8–24.
33. Pôças, I.; Paço, T.A.; Cunha, M.; Andrade, J.A.; Silvestre, J.; Sousa, A.; Santos, F.L.; Pereira, L.S.; Allen, R.G. Satellite based evapotranspiration of a super-intensive olive orchard: Application of METRIC algorithms. *Biosyst. Eng.* **2014**, *126*, 69–81.
34. Paredes, P.; Rodrigues, G.C.; Alves, I.; Pereira, L.S. Partitioning evapotranspiration, yield prediction and economic returns of maize under various irrigation management strategies. *Agric. Water Manag.* **2014**, *135*, 27–39.
35. Pereira, L.S.; Paredes, P.; Rodrigues, G.C.; Neves, M. Modeling malt barley water use and evapotranspiration partitioning in two contrasting rainfall years. Assessing AquaCrop and SIMDualKc models. *Agric. Water Manag.* **2015**, submitted.
36. Tasumi, M.; Allen, R.G.; Trezza, R. At-surface reflectance and albedo from satellite for operational calculation of land surface energy balance. *J. Hydrol. Eng.* **2008**, *13*, 51–63.

37. Chander, G.; Markham, B.L.; Helder, D.L. Summary of current radiometric calibration coefficients for Landsat MSS, TM, ETM+, and EO-1 ALI sensors. *Remote Sens. Environ.* **2009**, *113*, 893–903.
38. Chander, G.; Markham, B. Revised Landsat-5 TM radiometric calibration procedures and postcalibration dynamic ranges. *IEEE Trans. Geosci. Remote Sens.* **2003**, *41*, 2674–2677.
39. Rosa, R.D.; Paredes, P.; Rodrigues, G.C.; Fernando, R.M.; Alves, I.; Pereira, L.S.; Allen, R.G. Implementing the dual crop coefficient approach in interactive software: 2. Model testing. *Agric. Water Manag.* **2012**, *103*, 62–77.
40. Paço, T.; Ferreira, M.; Rosa, R.; Paredes, P.; Rodrigues, G.; Conceição, N.; Pacheco, C.; Pereira, L. The dual crop coefficient approach using a density factor to simulate the evapotranspiration of a peach orchard: SIMDualKc model *versus* eddy covariance measurements. *Irrig. Sci.* **2012**, *30*, 115–126.
41. Ding, R.; Kang, S.; Zhang, Y.; Hao, X.; Tong, L.; Du, T. Partitioning evapotranspiration into soil evaporation and transpiration using a modified dual crop coefficient model in irrigated maize field with ground-mulching. *Agric. Water Manag.* **2013**, *127*, 85–96.
42. Phogat V.; Skewes, M.A.; Mahadevan, M.; Cox, J.W. Evaluation of soil plant system response to pulsed drip irrigation of an almond tree under sustained stress conditions. *Agric. Water Manag.* **2013**, *118*, 1–11.
43. Santos, C.; Lorite, I.J.; Allen, R.G.; Tasumi, M. Aerodynamic Parameterization of the Satellite-Based Energy Balance (METRIC) Model for ET Estimation in Rainfed Olive Orchards of Andalusia, Spain. *Water Resour. Manag.* **2012**, *26*, 3267–3283.
44. Allen, R.G.; Pereira, L.S.; Smith, M.; Raes, D.; Wright, J. FAO-56 dual crop coefficient method for estimating evaporation from soil and application extensions. *J. Irrig. Drain. Eng.* **2005**, *131*, 2–13.
45. Zhao, N.; Liu, Y.; Cai, J.; Paredes, P.; Rosa, R.D.; Pereira, L.S. Dual crop coefficient modeling applied to the winter wheat—Summer maize crop sequence in North China Plain: Basal crop coefficients and soil evaporation component. *Agric. Water Manag.* **2013**, *117*, 93–105.
46. Wei, Z.; Paredes, P.; Liu, Y.; Chi, W.W.; Pereira, L.S. Modeling transpiration, soil evaporation and yield prediction of soybean in North China Plain. *Agric. Water Manag.* **2015**, *147*, 43–53.
47. Zhang, B.; Liu, Y.; Xu, D.; Zhao, N.; Lei, B.; Rosa, R.D.; Paredes, P.; Paço, T.A.; Pereira, L.S. The dual crop coefficient approach to estimate and partitioning evapotranspiration of the winter wheat—summer maize crop sequence in North China Plain. *Irrig. Sci.* **2013**, *31*, 1303–1316.
48. Calera Belmonte, A.; Jochum, A.M.; García, A.C. Space-assisted irrigation management: Towards user-friendly products. In Proceedings of ICID Workshop on Use of Remote Sensing of Crop Evapotranspiration for Large Regions, Montpellier, France, 17 September 2003.
49. Calera, A.; González-Piqueras, J.; Melia, J. Monitoring barley and corn growth from remote sensing data at field scale. *Int. J. Remote Sens.* **2004**, *25*, 97–109.
50. Duchemin, B.; Hadria, R.; Erraki, S.; Boulet, G.; Maisongrande, P.; Chehbouni, A.; Escadafal, R.; Ezzahar, J.; Hoedjes, J.C.B.; Kharrou, M.H.; *et al.* Monitoring wheat phenology and irrigation in Central Morocco: On the use of relationships between evapotranspiration, crops coefficients, leaf area index and remotely-sensed vegetation indices. *Agric. Water Manag.* **2006**, *79*, 1–27.

51. González-Dugo, M.P.; Mateos, L. Spectral vegetation indices for benchmarking water productivity of irrigated cotton and sugarbeet crops. *Agric. Water Manag.* **2008**, *95*, 48–58.
52. Stagakis, S.; González-Dugo, V.; Cid, P.; Guillén-Climent, M.L.; Zarco-Tejada, P.J. Monitoring water stress and fruit quality in an orange orchard under regulated deficit irrigation using narrow-band structural and physiological remote sensing indices. *ISPRS J. Photogramm. Remote Sens.* **2012**, *71*, 47–61.
53. Kohavi, R. A study of cross-validation and bootstrap for accuracy estimation and model selection. In Proceedings of the Fourteenth International Joint Conference on Artificial Intelligence, Montreal Quebec, Canada, 20–25 August, 1995; Morgan Kaufman Publishers Inc.: San Francisco, CA, USA; pp. 1137–1143.
54. Cunha, M.; Marçal, A.R.S.; Silva, L. Very early prediction of wine yield based on satellite data from VEGETATION. *Int. J. Remote Sens.* **2010**, *31*, 3125–3142.
55. Lindberg, E.; Holmgren, J.; Olofsson, K.; Wallerman, J.; Olsson, H. Estimation of tree lists from airborne laser scanning using tree model clustering and k-MSN imputation. *Remote Sens.* **2013**, *5*, 1932–1955.
56. Trout, T.J.; Johnson, L.F.; Gartung, J. Remote sensing of canopy cover in horticultural crops. *HortScience* **2008**, *43*, 333–337.
57. Purevdorj, T.S.; Tateishi, R.; Ishiyama, T.; Honda, Y. Relationships between percent vegetation cover and vegetation indices. *Int. J. Remote Sens.* **1998**, *19*, 3519–3535.
58. Carreiras, J.M.B.; Pereira, J.M.C.; Pereira, J.S. Estimation of tree canopy cover in evergreen oak woodlands using remote sensing. *For. Ecol. Manag.* **2006**, *223*, 45–53.
59. Gonzalez-Piqueras, J.; Calera Belmonte, A.; Gilabert, M.A.; Cuesta García, A.; de la Cruz Tercero, F. Estimation of crop coefficient by means of optimized vegetation indices for corn. *Proc. SPIE* **2004**, *5232*, doi:10.1117/12.511317.
60. Bausch, W.C. Soil background effects on reflectance-based crop coefficients for corn. *Remote Sens. Environ.* **1993**, *46*, 213–222.
61. Hunsaker, D.J.; Fitzgerald, G.J.; French, A.N.; Clarke, T.R.; Ottman, M.J.; Pinter, P.J., Jr. Wheat irrigation management using multispectral crop coefficients: I. Crop evapotranspiration prediction. *Trans. ASAE* **2007**, *50*, 2017–2033.
62. Liu, Z.; Yao, Z.; Yu, C.; Zhong, Z. Assessing crop water demand and deficit for the growth of spring highland barley in Tibet, China. *J. Integr. Agric.* **2013**, *12*, 541–551.
63. Villalobos, F.J.; Orgaz, F.; Testi, L.; Fereres, E. Measurement and modeling of evapotranspiration of olive (*Olea europaea* L.) orchards. *Eur. J. Agron.* **2000**, *13*, 155–163.